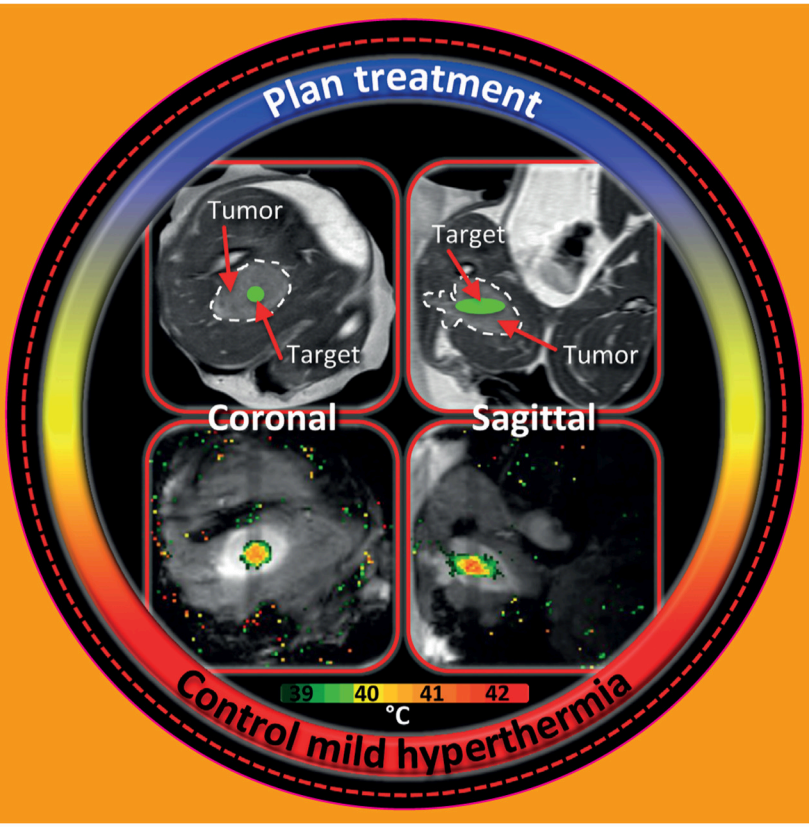

Report Series in Physics
HU-P-D204

MAGNETIC RESONANCE-GUIDED HIGH-INTENSITY FOCUSED ULTRASOUND MEDIATED MILD HYPERTHERMIA AND DRUG DELIVERY

Ari Partanen

UNIVERSITY OF HELSINKI REPORT SERIES IN PHYSICS

HU-P-D204

Magnetic resonance-guided high-intensity focused ultrasound mediated mild hyperthermia and drug delivery

Ari Ilkka Mikael Partanen

Department of Physics
Faculty of Science
University of Helsinki
Helsinki, Finland

ACADEMIC DISSERTATION FOR THE DEGREE OF DOCTOR OF PHILOSOPHY

To be presented, with the permission of the Faculty of Science of the University of Helsinki, for public examination in Auditorium A110 (Chemicum, A.I. Virtasen aukio 1, Helsinki, Finland) on the 14th of June, 2013, at 12 noon.

Helsinki, 2013

SUPERVISED BY

Prof. Sauli Savolainen, Ph.D.
Department of Physics
University of Helsinki
Finland

HUS Medical Imaging Center
Helsinki University Central Hospital
Finland

PRE-EXAMINED BY

Prof. Raimo Sepponen, D.Sc. (EE)
Department of Electronics
Aalto University
Finland

Prof. Jukka Jurvelin, Ph.D.
Department of Applied Physics
University of Eastern Finland
Finland

OPPONENT

Prof. Kullervo Hynynen, Ph.D.
Department of Medical Biophysics and Institute of
Biomaterials and Biomedical Engineering
Canada Research Chair in Imaging Systems and
Image-Guided Therapy (Tier 1)
University of Toronto
Canada

ISBN 978-952-10-8094-4 (pbk.)
Helsinki University Print
Helsinki, 2013

ISBN 978-952-10-8095-1 (PDF)
Helsinki University E-thesis
http://ethesis.helsinki.fi
Helsinki, 2013

A. Partanen: Magnetic resonance-guided high-intensity focused ultrasound mediated mild hyperthermia and drug delivery, University of Helsinki, 2013, 56 pp. + appendices 85 pp. University of Helsinki Report Series in Physics, HU-P-D204, ISSN 0356-0961, ISBN 978-952-10-8094-4

Keywords: thermotherapy, hyperthermia, high-intensity focused ultrasound, magnetic resonance imaging, MR-HIFU, MRI, thermometry, drug delivery, thermosensitive liposome, feedback control

Abstract

Ablative hyperthermia (> 55 °C) has been used as a stand-alone treatment for accessible solid tumors not amenable to surgery, whereas mild hyperthermia (40–45 °C) has been shown effective as an adjuvant for both radiotherapy and chemotherapy. An optimal mild hyperthermia treatment is noninvasive and spatially accurate, with precise and homogeneous heating limited to the target region and with reduced probability of unwanted thermal or mechanical bioeffects (tissue damage, vascular shutoff). High-intensity focused ultrasound (HIFU) can noninvasively heat solid tumors deep within the human body. Magnetic resonance imaging (MRI) is ideal for HIFU treatment planning and monitoring in real time due to its superior soft-tissue contrast, high spatial imaging resolution, and the ability to measure temperature changes. The combination of HIFU therapy and MRI monitoring is called magnetic resonance-guided high-intensity focused ultrasound (MR-HIFU).

Low temperature-sensitive liposomes (LTSLs) release their drug cargo in response to heat (> 40 °C) and may improve drug delivery to solid tumors when combined with mild hyperthermia. MR-HIFU provides a way to image and control content release from imageable low-temperature sensitive liposomes (iLTSLs). This ability may enable spatiotemporal control over drug delivery — a concept known as drug dose painting. In this paradigm, the treating physician prescribes a desired drug dose and spatial distribution of drug to be delivered, and an MR-HIFU system manipulates heat in the target region to achieve the desired drug dose.

The objectives of this dissertation were to develop and implement a clinically relevant volumetric mild hyperthermia heating algorithm, to implement and characterize different sonication approaches (multiple foci vs. single focus), and to evaluate the ability to monitor and control heating in real time with MR-HIFU. In addition, the ability of MR-HIFU to induce the release of a clinical-grade cancer drug encapsulated in LTSLs was investigated, and the potential of MR-HIFU mediated mild hyperthermia for clinical translation as an image-guided drug delivery method was explored. Finally, drug and contrast agent release of iLTSLs as well as the ability of MR-HIFU to induce and monitor the content release were examined, and a computational model that simulates MR-HIFU tissue heating and the resulting hyperthermia-mediated drug delivery was validated.

The developed MR-HIFU mild hyperthermia heating algorithm produced accurate and homogeneous heating within the targeted region *in vitro* and *in vivo*. The combination of a multifoci sonication approach and the mild hyperthermia heating algorithm resulted in accurate and precise heating within the targeted region with significantly lower acoustic pressures. Heating was more spatially confined in the beam path direction compared to the use of single focus sonication method. The reduction in acoustic pressure and improvement in spatial control suggest that multifoci heating is a useful tool in MR-HIFU mediated mild hyperthermia applications for clinical oncology.

Using the mild hyperthermia heating algorithm, LTSL + MR-HIFU resulted in significantly higher tumor drug concentrations compared to free drug and LTSL alone. This technique has potential for clinical translation as an image-guided method to deliver drug to a solid tumor. MR-HIFU also enabled real-time monitoring and control of iLTSL content release. Finally, computational models can predict temperature distribution and delivered drug concentration resulting from combining MR-HIFU with LTSLs, and may allow quantitative *in silico* comparison of different MR-HIFU heating algorithms as well as facilitate therapy planning for this drug delivery technique.

Preface

The work presented herein has been performed at the National Institutes of Health (Bethesda, MD, USA) during the years 2009-2012, in close collaboration with Philips Healthcare as well as with Department of Physics at the University of Helsinki.

First and foremost, I would like to thank my advisors Dr. Matthew Dreher and Dr. Gösta Ehnholm, as well as my supervisor Prof. Sauli Savolainen for their words of wisdom, support, and guidance during all stages of this work. I furthermore wish to thank the head of the physics department, Prof. Juhani Keinonen, for his aid and support in all academic matters. Pre-examiners Prof. Raimo Sepponen and Prof. Jukka Jurvelin are in turn appreciated for their careful review and constructive criticism.

I also express my sincere appreciation to my lab mates and co-authors Pavel Yarmolenko, Ayele Negussie, David Woods, Dr. Bradford Wood, Dr. Dieter Haemmerich, Dr. Astrid Gasselhuber, Dr. Ashish Ranjan, Genevieve Jacobs, Antti Viitala, Sunil Appanaboyina, Matti Tillander, Dr. Sham Sokka, Julia Enholm, Dr. Max Köhler, Dr. Carmen Gacchina, Dr. Karun Sharma, Dr. Raja Muthupillai, Dr. Caitlin Burke, and Dr. Aradhana Venkatesan, who have supported and assisted me in this research and with experimentation.

I further wish to thank all my colleagues at Philips Healthcare for their help and advice given throughout this research, and for encouraging the writing of this dissertation.

Above all, I wish to express my gratitude to my parents Liisa and Per-Olof and to my brother Anssi for their continual care and encouragement. I would not be where I am today without their support.

Finally, I have been extremely fortunate to have the support of exceptional friends to whom I am truly grateful. Thank you for the good times. You know who you are.

This research was supported by the Center for Interventional Oncology and Intramural Research Program of the National Institutes of Health, and through a Cooperative Research and Development Agreement with Philips Healthcare.

Ari Partanen

1st of May, 2013, Bethesda, MD, USA

Table of contents

List of original publications

This dissertation consists of an overview to MR-HIFU mediated mild hyperthermia and drug delivery, and of six original publications that are listed below in logical order and referred to by their Roman numerals in the overview.

I Partanen A, Yarmolenko PS, Viitala A, Appanaboyina S, Haemmerich D, Ranjan A, Jacobs G, Woods D, Enholm J, Wood BJ, Dreher MR. *"Mild hyperthermia with magnetic resonance-guided high-intensity focused ultrasound for applications in drug delivery,"* Int J Hyperthermia. 2012;28(4):320-36.

II Partanen A, Tillander M, Yarmolenko PS, Wood BJ, Dreher MR, Köhler MO. *"Reduction of peak acoustic pressure and shaping of heated region by use of multifoci sonications in MR-guided high-intensity focused ultrasound mediated mild hyperthermia,"* Med Phys. 2013 Jan;40(1):013301.

III Ranjan A, Jacobs GC, Woods DL, Negussie AH, Partanen A, Yarmolenko PS, Gacchina CE, Sharma KV, Frenkel V, Wood BJ, Dreher MR. *"Image-guided drug delivery with magnetic resonance guided high intensity focused ultrasound and temperature sensitive liposomes in a rabbit Vx2 tumor model,"* J Control Release. 2012 Mar 28;158(3):487-94.

IV Negussie AH, Yarmolenko PS, Partanen A, Ranjan A, Jacobs G, Woods D, Bryant H, Thomasson D, Dewhirst MW, Wood BJ, Dreher MR. *"Formulation and characterisation of magnetic resonance imageable thermally sensitive liposomes for use with magnetic resonance-guided high intensity focused ultrasound,"* Int J Hyperthermia. 2011;27(2):140-55.

V Gasselhuber A, Dreher MR, Partanen A, Yarmolenko PS, Woods D, Wood BJ, Haemmerich D. *"Targeted drug delivery by high intensity focused ultrasound mediated hyperthermia combined with temperature-sensitive liposomes: computational modelling and preliminary in vivo validation,"* Int J Hyperthermia. 2012;28(4):337-48.

VI Venkatesan AM, Partanen A, Pulanic TK, Dreher MR, Fischer J, Zurawin RK, Muthupillai R, Sokka S, Nieminen HJ, Sinaii N, Merino M, Wood BJ, Stratton P. *"Magnetic resonance imaging-guided volumetric ablation of symptomatic leiomyomata: correlation of imaging with histology,"* J Vasc Interv Radiol. 2012 Jun;23(6):786-794.

Author's contributions

Publication **I** presents a binary feedback algorithm for MR-HIFU mediated volumetric mild hyperthermia. Performance of MR-HIFU feedback-controlled mild hyperthermia was evaluated both *in vitro* and *in vivo* using a clinical MR-HIFU platform. Furthermore, the spatiotemporal temperature accuracy and uniformity, as well as spatial targeting accuracy and sonication efficiency were critically assessed. The author had a key role in the design, development, and testing of the mild hyperthermia feedback control strategy, for which a patent was filed. The author also took primary responsibility of the control of the MR-HIFU system, optimized the sonication and imaging parameters, carried out the in vitro experiments, participated in all of the animal experiments, and performed the data analysis. In addition, the author was responsible for the production of the manuscript.

In publication **II**, a multifoci sonication approach for feedback-controlled MR-HIFU mediated mild hyperthermia was developed and combined with the mild hyperthermia heating algorithm presented in publication **I** on a clinical MR-HIFU platform. Feasibility of this sonication strategy was tested and verified *in silico*, in acoustic hydrophone measurements, *in vitro*, and *in vivo*. Performance of the system was characterized in terms of temperature uniformity, spatial control of temperature, as well as acoustic pressure and intensity in the target region. The author significantly contributed to the development of this sonication approach (for which a patent was filed), implemented this strategy on a clinical MR-HIFU platform, and performed the *in vitro* and *in vivo* experiments and the corresponding data analysis. Furthermore, the author had primary responsibility for the construction of the manuscript.

In publication **III,** the feedback algorithm developed in publication **I** was applied to *in vivo* drug delivery studies using low-temperature sensitive liposomes (LTSL). Improved tumor drug concentration resulting from the combination of MR-HIFU and LTSL was shown, and the feasibility of MR-HIFU mediated drug delivery was examined and discussed. The author participated in all the animal experiments, was in control of the MR-HIFU system operation, and made significant contributions to data analysis and manuscript production, especially regarding data presentation.

Publication **IV** describes the development and characterization of an MR-imageable low-temperature sensitive liposome (iLTSL) formulation co-loaded with a cancer drug and an MR contrast agent, and its application *in vivo* using MR-HIFU. Liposome stability and imageability, as well as MR-HIFU monitoring and control of content release were assessed. The author had primary responsibility over the MR- and MR-HIFU experiments, and contributed extensively to data analysis and manuscript creation.

Publication **V** portrays the use of computational models in predicting temperature distribution and delivered drug concentration from the combination of MR-HIFU mediated hyperthermia and LTSLs. The author was responsible for the control of the MR-HIFU system in the *in vivo* experiment, in which the feedback algorithm and imaging protocols from publication **I** were used. In addition, the author made significant contributions to the manuscript, especially regarding analysis and presentation of the experimental data.

Publication **VI** depicts MR-HIFU volumetric ablation of symptomatic uterine leiomyomata, and the correlation of post-treatment contrast-enhanced imaging with histology. Treatment safety profile and spatial accuracy of the ablations were evaluated, imaging findings and pathologic confirmation of ablation were assessed, and the novel treatment control and monitoring capabilities of MR-HIFU were discussed. The author participated in all of the patient treatments, and had responsibility over the operation of the MR-HIFU system. In addition, the author contributed greatly to the manuscript, especially regarding the data analysis as well as data presentation.

List of abbreviations

2D	Two-dimensional
3D	Three-dimensional
ANOVA	Analysis of variance, a statistical test
BHTE	Bioheat transfer equation
CEI	Contrast-enhanced imaging
CEM_{43}	Cumulative equivalent minutes at 43 °C, a unit of thermal dose
CRADA	Cooperative research and development agreement
DDS	Drug delivery system
DNA	Deoxyribonucleic acid
DOX	Doxorubicin, a cancer drug
DWI	Diffusion-weighted imaging
EES	Extracellular-extravascular space
EPI	Echo planar imaging, an MR-imaging technique
EPR	Enhanced permeability and retention
FA	Flip angle, an MRI scan parameter
FDA	Food and drug administration, a government agency in the USA
FFE	Fast field echo, an MR-imaging method
FOV	Field of view
Gd-DTPA	Gadopentetic acid, a paramagnetic contrast agent for MRI
HIFU	High-intensity focused ultrasound
HT	Hyperthermia
iLTSL	Imageable low-temperature sensitive liposome
LTSL	Low-temperature sensitive liposome
MR-HIFU	Magnetic resonance-guided high-intensity focused ultrasound
MRI	Magnetic resonance imaging
NIH	National Institutes of Health
NMR	Nuclear magnetic resonance
PI	Proportional-integral, usually refers to a control algorithm
PID	Proportional-integral-derivative, a control algorithm
PRFS	Proton resonance frequency shift
RF	Radio frequency
RNA	Ribonucleic acid
SNR	Signal-to-noise ratio
TD_{43}	Thermal dose in equivalent minutes at 43 °C
TE	Echo time, an MRI scan parameter
TR	Repetition time, an MRI scan parameter
TSL	Temperature sensitive liposome
Vx2	Squamous cell carcinoma rabbit tumor model

List of symbols

^{1}H	A hydrogen isotope
B_0	Main magnetic field
B_{loc}	Local magnetic field
c	Speed of sound
c_{bl}	Specific heat capacity of blood
c_t	Specific heat capacity of tissue
f	Ultrasound frequency
f_0	Larmor resonance frequency
I	Acoustic intensity
k_t	Thermal conductivity of tissue
N	Number of transducer elements
p	Acoustic pressure
P_{ac}	Acoustic power
Q_{HIFU}	External heat source term / tissue energy absorption
T_1	Longitudinal relaxation time
T_{10}	The 10th percentile
T_2	Transverse relaxation time
T_{90}	The 90th percentile
T_{bl}	Arterial blood temperature
T_{ref}	Reference temperature
w_{bl}	Blood perfusion rate
α	Ultrasound attenuation
α_T	Temperature-dependent part of chemical shift
γ	Gyromagnetic ratio
δ	Chemical shift
δ_0	Temperature-independent part of chemical shift
ΔT	Temperature change
θ	Flip angle
λ	Ultrasound wavelength
ρ_{bl}	Mass density of blood
ρ_t	Mass density of tissue
σ	Molecular shielding
Φ	MR image phase

1 Introduction

1.1 Cancer therapies and mild hyperthermia

Cancer is a term used for diseases in which anomalous cells divide and grow uncontrollably, possibly resulting in invasion of other tissues. [1, 2] Therapies for cancer can be roughly divided into five categories: surgery, chemotherapy, radiotherapy, transplantation, and other treatment methods, which include angiogenesis inhibitors, photodynamic therapy, cancer vaccines, gene therapy, and hyperthermia. [2] The choice of cancer therapy depends on the location and type of the tumor, the stage of the disease, as well as on the general well-being of the patient. [2]

Mild hyperthermia, i.e., exposing tissue to temperatures slightly above normal body temperature, is a therapeutic technique that is used as an adjuvant or neo-adjuvant therapy in combination with other forms of cancer therapy such as radiotherapy and chemotherapy. [3-5] In contrast, ablative hyperthermia is intended to directly produce substantial cell death at temperatures commonly greater than 55 °C. [6]

The goal of mild hyperthermia therapy is to obtain temperatures of 40–45 °C within the target tissue for time periods up to one hour. [3, 4] Hyperthermia treatments may result in both physiological (e.g., perfusion) and cellular (e.g., gene expression) changes that improve therapeutic effectiveness of chemotherapy and radiotherapy. [3] For example, mild hyperthermia may make cancer cells more sensitive to radiation or directly injure cancer cells, as well as enhance the effects of some cancer drugs. [3]

A number of clinical trials have studied mild hyperthermia in combination with radiotherapy and/or chemotherapy. These studies have focused on treatment of many types of cancer, showing that addition of mild hyperthermia can help provide palliative relief, as well as augment tumor response, local control, and survival. [3, 4, 7-9]

1.2 Mild hyperthermia mediated drug delivery

Current cancer therapies utilizing chemotherapeutic agents usually rely on systemic delivery with limited tumor specificity, and consequently may result in adverse side effects in healthy tissues and insufficient drug delivery to the target tumor. [10-12] In order to reduce systemic toxicity and improve overall efficacy, hyperthermia has been recently used in combination with temperature-responsive and non-temperature-responsive drug delivery systems (DDS). [13]

For non-temperature-responsive DDS, mild hyperthermia has been shown to assist drug delivery with stealth liposomes by increasing vascular permeability, resulting in enhanced drug levels in solid tumors, [14, 15] and may also increase the sensitivity of cancer cells to chemotherapeutics. [13] When hyperthermia is combined with temperature-responsive DDS, the heat may also be used as a trigger to initiate drug release. Temperature responsive DDS include polymers, [16] biopolymers, [17] micelles, [18] and liposomes. [19] One of the most promising temperature-responsive DDS are temperature sensitive liposomes (TSLs) that release their contents in response to temperatures greater than the melting temperature of the lipid formulation. [19, 20] Encapsulation of a chemotherapeutic agent into liposomes has the potential to reduce systemic toxicity and enhance drug delivery compared with free drug.

In recent times, low temperature sensitive liposomes (LTSLs) have been developed. [21, 22] These liposomes rapidly release the encapsulated cancer drug (e.g., doxorubicin) at mild hyperthermia (40–42 °C). [23-25] Studies combining LTSLs with local, mild hyperthermia have demonstrated significant tumor volume reduction in mouse tumor models compared with conventional free drug or non-thermally sensitive liposome therapies. [21, 22, 26, 27]

Intra- and inter-patient spatial variability in tumor microenvironment may impact both the heating pattern and delivery of drugs. [28, 29] To accommodate this variability, mild hyperthermia treatment may be adjusted for optimal drug delivery by using a control algorithm. Therefore, in addition to temperature monitoring, direct imaging of drug delivery (or an appropriate substitute, such as release of a contrast agent from LTSLs) may improve real-time control of delivery or help guide future interventions. A suitable surrogate for quantification of drug delivery may be provided by imaging contrast agent release from liposomes co-loaded with a drug and a contrast agent. [30]

Contrast agents have been encapsulated in liposome interior compartment [31] as well as conjugated to their membrane, [32] or both. [33] LTSLs that release contrast agent from their interior have been used to monitor release *in vivo*, and such liposomes have demonstrated promising correlations of imaging with both drug delivery [34] and therapeutic efficacy. [30]

1.3 Magnetic resonance-guided high-intensity focused ultrasound

Several methods for providing local, mild hyperthermia have been studied using techniques that deliver energy to a small volume, such as a tumor. [3, 7-9] Traditional hyperthermia applicators include radiofrequency, [35, 36] microwave, [37] hot water baths, [38] lasers, [39] and magnetic fluids. [40, 41] Despite some promising results, these methods suffer from drawbacks such as highly invasive nature of applicators, limited and superficial heating, formation of hot spots, inaccurate or spatially uneven heating, inability to achieve mild hyperthermic temperatures (40–45 °C), and lack of spatiotemporal temperature feedback control. [3]

High-intensity focused ultrasound (HIFU) utilizes tightly focused ultrasonic waves, leading to absorption of energy and rapid, highly localized temperature elevations at the target. HIFU represents a noninvasive alternative to more widely used hyperthermia applicators. Application of HIFU can result in both thermal and non-thermal (often known as mechanical) bioeffects, both of which arise from a complex interaction of propagating ultrasound waves with tissue. [42-44] Importantly, HIFU bioeffects can be manipulated and/or controlled by adjusting device output power, ultrasound frequency, duty cycle, sonication duration, and focal spot characteristics.

Although focused ultrasound was suggested for localized hyperthermia and noninvasive surgery as early as in the 1940s, [45] the lack of suitable image guidance and temperature control techniques prevented it from gaining widespread clinical adoption. [46] Due to its superior soft-tissue contrast, high spatial image resolution, and the ability to monitor temperature changes, magnetic resonance imaging (MRI) is uniquely qualified to provide both HIFU treatment planning as well as real-time monitoring of therapy. The combination of HIFU therapy and MRI monitoring is called magnetic resonance-guided high-intensity focused ultrasound (MR-HIFU). Temperature monitoring with MRI is commonly achieved using the water proton resonance frequency shift (PRFS) method, [47] which relies on the linear dependence of PRFS on temperature change. In the mild hyperthermic range, this linear relationship is valid in all non-adipose tissues. [48] The PRFS method has been used to provide accurate and real-time thermometry free of interference from HIFU. [48-53]

To date, clinical MR-HIFU has been mostly used for the ablation of symptomatic uterine leiomyomata, [50, 52, 54-56] which are common benign smooth-muscle tumors located within the uterus. MR-HIFU also shows promise for oncology applications, and it has been under investigation for the treatment of benign breast fibroadenomas, [57] malignant breast carcinoma, [58, 59] prostate cancer, [60, 61] palliative treatment of painful osseous metastases, [62-64] and for the ablation of brain tumors. [65, 66] In addition, MR-HIFU is currently under research for the treatment of neurological disorders, including epilepsy, essential tremor, neuropathic pain, and Parkinson's disease. [67-69]

Developments in both ultrasound applicators and MRI-based temperature monitoring and control methods [48, 51, 70-74] have made MR-HIFU mediated mild hyperthermia an attractive option as a noninvasive hyperthermia therapy modality, especially in combination with drug delivery.

1.4 Feedback controlled mild hyperthermia and drug delivery using magnetic resonance-guided high-intensity focused ultrasound

The efficacy of a mild hyperthermia treatment is associated with the temperatures achieved during the treatment, duration of treatment, as well as cell and tissue characteristics. [3, 7, 75] An optimal mild hyperthermia treatment is spatially accurate, with precise and homogeneous heating limited to the target region and with low likelihood of unwanted thermal or mechanical bioeffects (direct tissue damage, vascular shutoff). The ideal temperature for most mild hyperthermia applications is 40–45 °C (T < 40 °C causes limited effect, T > 45 °C may shut down tissue perfusion [3, 76]), and may require durations of 30–60 min, [76] placing strict and challenging requirements on both the hyperthermia applicator and delivery approaches.

Phased-array ultrasound transducers in combination with suitable driving electronics make the creation of different focal patterns possible by enabling fast temporal displacement of the focus or the generation of multiple foci, thus significantly increasing the heated volume. [51, 77-79] To ensure that the desired temperature is reached but not exceeded in the target volume, the temperature of the tumor and surrounding tissue must be monitored and controlled throughout a mild hyperthermia treatment. MRI thermometry can be utilized to perform either operator-adjustable or automated feedback control of the treatment in order to improve temperature accuracy and uniformity, as well as patient safety. [23, 73, 80-83]

1.5 Context of dissertation

The work performed for this dissertation was part of a collective effort to develop, characterize, and validate methods and materials for safe, targeted, and noninvasive MR-HIFU mediated mild hyperthermia and drug delivery therapies.

Locally targeted, image-guided mild hyperthermia, as well as drug delivery assisted by mild hyperthermia are clinically attractive and potentially useful strategies for enhancing cancer therapies and augmenting delivery of drugs to solid tumors. However, for these strategies to realize their full potential in the clinic, a hyperthermia applicator must be able to provide accurate and homogenous heating in a target volume. In this dissertation work, novel methods for MR-HIFU mediated mild hyperthermia and drug delivery have been developed and characterized for use with a clinical MR-HIFU system. The key results of the related research and the relevant scientific background are portrayed in this dissertation. This research is presented in publications **I**-**IV**.

A variety of factors, including drug delivery system, drug characteristics, as well as physiological, biological, and biophysical parameters, affect hyperthermia-mediated drug delivery from LTSLs. Computer simulations may provide a means to efficiently study the effects of these parameters. Other benefits offered by computer simulations include facilitating detailed examination of heating algorithms and optimal drug delivery strategies. This dissertation also describes evaluation of a computational model that simulates tissue heating with MR-HIFU as well as the resulting mild hyperthermia assisted drug delivery from LTSLs. This research is presented in publication **V**.

Finally, the use of MR-HIFU for the ablation of symptomatic uterine leiomyomata is presented in publication **VI**. This publication showcases that combining HIFU therapy with novel MRI-based treatment monitoring and control is not only feasible, but already in clinical use with impressive targeting accuracy and an acceptable treatment safety profile.

The overview part of this dissertation includes three chapters focusing on MR-HIFU mediated mild hyperthermia and drug delivery. Tissue effects of mild hyperthermia and its use in cancer treatments, as well as mild hyperthermia mediated drug delivery, are presented in Chapter 2. The basics of therapeutic ultrasound, interaction of HIFU with tissue, as well as methods for delivering acoustic energy using different sonication strategies for HIFU are described in Chapter 3. Means for MRI-based treatment planning, temperature monitoring, and therapy assessment are described in Chapter 4.

Furthermore, the objectives of this dissertation work are outlined below and the fulfillment of these objectives is discussed in Chapter 5. Finally, key results of the six publications are briefly summarized in Chapter 6.

Objectives

1. Develop and implement a clinically relevant volumetric mild hyperthermia heating algorithm and evaluate its ability to monitor and control heating in real time using a clinical MR-HIFU system. (**I**)
2. Implement and characterize a multifoci sonication approach in combination with the mild hyperthermia heating algorithm developed under objective 1, and compare it to the more conventional method of electronically sweeping a single focus. (**II**)
3. Investigate the ability of MR-HIFU to induce the release of a clinical-grade cancer drug encapsulated in LTSLs, and explore the potential of MR-HIFU mediated mild hyperthermia for clinical translation as an image-guided drug delivery method. (**III**)
4. Characterize the drug and contrast agent release of iLTSLs, and investigate the ability of MR-HIFU to induce and monitor the content release. (**IV**)
5. Validate a computational model that simulates MR-HIFU mediated tissue heating and the resulting mild hyperthermia assisted drug delivery from LTSLs. (**V**)

In addition, the objective of publication **VI** was to show that MR-HIFU therapy for the ablation of symptomatic uterine leiomyomata is not only feasible, but already in clinical use with impressive targeting accuracy and an acceptable treatment safety profile.

2 Mild hyperthermia therapy and mild hyperthermia mediated drug delivery

2.1 Mild hyperthermia therapy

Mild hyperthermia is a therapeutic technique, in which cancerous tissue is heated above the body temperature (40–45 °C for up to 1 hour) in order to induce a physiological or biological effect. [3, 4] Usually, the goal of mild hyperthermia is to improve the therapeutic effectiveness of chemotherapy or radiotherapy, and it is not typically intended to directly produce substantial cell death. In contrast, ablative hyperthermia commonly achieves temperatures greater than 55 °C, but for shorter durations of 20 s to 15 min, [6] with a primary goal of ensuring cancer cell death.

The beneficial effects of mild hyperthermia lie in its ability to improve the effectiveness of other treatments by modifying both physiology and biology of cancer. [3, 8, 9] Mild hyperthermia may provide improved tissue perfusion and oxygenation, [3] inhibit homologous recombination, [84] improve delivery of chemotherapy and potentiate its cytotoxic effects, [3] as well as augment immune response. [85] Culmination of these effects has promising potential to improve outcomes for cancer patients who receive radio- and/or chemotherapy.

2.2 Delivery methods for mild hyperthermia

Delivery methods include local, regional, and whole-body mild hyperthermia. [5, 7, 75] Whole-body mild hyperthermia has been investigated as a treatment for metastatic cancer that has spread throughout the body. Techniques include infrared hyperthermia domes, placing the patient in a very hot room, or wrapping the patient in hot, wet blankets. [5, 7] The application of whole-body mild hyperthermia is accompanied with a wider range of toxic side effects than other mild hyperthermia modalities. [75]

Regional mild hyperthermia may be applied with a variety of approaches to selectively heat volumes of tissue with variable size and morphology, such as a tumor and surrounding tissue, a body cavity, organ, or an entire limb. For example, regional perfusion techniques can be used to treat cancers in the extremities (e.g., melanoma) or cancer in some organs, such as in the liver or lung. In these procedures, the target limb or organ is perfused with the patient's own blood that has been diverted and continuously circulated through a heating apparatus. [7, 75]

In local hyperthermia, heat is applied to a small volume using different types of applicators, such as radiofrequency, [35, 36] microwave, [37] laser, [39] and ultrasound. [86, 87] The choice of heating method for local mild hyperthermia is dictated largely by the tumor location. External approaches are typically used to treat tumors that are in or just below the skin. Endocavitary methods are used to treat tumors within or near body cavities, such as the esophagus or rectum. Interstitial techniques are used to treat tumors deep within the body, such as brain tumors. [3, 7, 9]

What all mild hyperthermia modalities have in common is that they are typically used to improve the therapeutic effectiveness when used as an adjuvant or neo-adjuvant therapy, and not intended to replace any of the established oncological treatment modalities. There are a number of technological challenges that make mild hyperthermia therapy complicated and that have barred mild hyperthermia from becoming a more widely used treatment option in clinical practice. These challenges include applicators that are hard to use or control, the ability to achieve a uniform temperature in a tumor, and the ability to precisely monitor temperature both within the tumor and in the surrounding tissue. Applicators and methodology to deliver uniform levels of thermal energy, as well as devices to monitor and control the total amount of delivered energy, are therefore desirable.

2.3 Tissue effects of mild hyperthermia

Exposure to hyperthermic temperatures has been shown to damage DNA, RNA, proteins, nucleoproteins, chromosomes, lipids, nucleoli, membranes, lysosomes, microtubules, as well as a large variety of synthetic pathways and metabolic functions within the cell. [3, 75, 88] Thus, hyperthermia affects practically all cell structures and functions.

In more detail, mild hyperthermia has been shown to play a role in changing the stability and fluidity of cell membranes, [89, 90] altering cell shape, [5, 91] inducing apoptosis, [92] impairing protein synthesis, [5, 93] denaturing proteins, [94, 95] inducing heat-shock protein synthesis, [95, 96] as well as in decreasing RNA/DNA synthesis and inhibiting repair enzymes. [5, 93, 97] Furthermore, mild hyperthermia may affect drug distribution by altering tumor blood flow [5, 98, 99] or by increasing the enhanced permeability and retention (EPR) effect. [10, 14, 100-102]

These effects may also lead to altered interactions between heat and drugs. For example, mild hyperthermia may affect pharmacodynamics by accelerating the primary mode of action of cancer therapies (e.g., DNA-strand breaks, protein damage), or by other means, such as increasing intracellular drug concentration through membrane and protein damage. [75] A thorough review on the cellular and molecular effectors of mild hyperthermia as well as on the interactions between heat and drugs has been previously published by Hildebrandt et al. [75]

2.4 Mild hyperthermia in cancer treatments, and the clinical effectiveness of mild hyperthermia

A number of clinical trials have examined the safety and efficacy of mild hyperthermia in combination with radiotherapy and/or chemotherapy. [3, 7, 75] These studies have focused on the treatment of many types of cancer, including sarcoma, melanoma, cancers of the head and neck, brain, lung, esophagus, breast, bladder, rectum, liver, appendix, cervix, and peritoneal lining. [3, 4, 7-9, 75] Many of these trials have shown a significant reduction in tumor size when mild hyperthermia is combined with other treatments. [3, 7, 8] These findings strongly suggest the clinical effectiveness of hyperthermia, [4, 103-108] and as such, the principal argument for the use of mild hyperthermia is its proven benefit in the scope of randomized clinical trials.

Radiotherapy uses high-energy radiation to kill cancer cells by damaging their DNA, resulting in reduction of tumor size. [109] X-rays, gamma rays, and charged particles are common types of radiation used in cancer treatments. Radiation may be delivered by a machine outside the body, [109] or it may arise from radioactive material placed in the body near tumor cells or injected into the bloodstream. [110]

An important observation based on both *in vitro* and *in vivo* studies on thermal therapies is that mild hyperthermia and radiation provide complementary effects and act in a synergistic way, significantly increasing tumor cell death over levels achieved with radiation alone. [3, 75] This mild hyperthermia-mediated thermal radiosensitization (thermoradiosensitization) appears most pronounced for cells in synthesis-phase (DNA replication phase) of the cell cycle. These cells are usually less affected by radiation alone, but are the most sensitive to hyperthermia. [111, 112] However, the greatest impact of mild hyperthermia is likely on cells that have been deprived of oxygen. A growing tumor rapidly outgrows its blood supply, leaving regions in the tumor with significantly lower oxygen concentration compared to healthy tissue. This condition is called tumor hypoxia. Hypoxic tumor cells may be resistant to radiotherapy and chemotherapy, [113] but they can be made more amenable to treatment if delivery of oxygen is improved. The documented ability of mild hyperthermia to improve tumor oxygenation [114] may account for its enhancement of radio- and chemo-sensitization. [115]

Improved response and survival rates have been observed in patients treated with mild hyperthermia and radiotherapy compared with radiotherapy alone in multiple phase III trials. [116-122] Despite the inhomogeneity of achieved temperature distribution, the use of local and/or regional mild hyperthermia techniques indicated a significant correlation between thermal dose and clinical outcome in some of these trials. [105, 123, 124] In summary, data from both pre-clinical and clinical studies indicate that therapeutic outcomes may be improved by using the combination of mild hyperthermia and radiotherapy.

Chemotherapy is a type of cancer treatment that uses drugs to destroy cancer cells. Chemotherapy works by stopping or slowing the progression of cancer cells, which typically grow and divide rapidly. [2] However, chemotherapy targets all rapidly dividing cells — normal cells and cancer cells alike. Thus, chemotherapy can harm healthy cells that divide quickly, e.g., cells in intestinal lining, bone marrow, or in hair follicles, causing unwanted side effects such as alopecia and neutropenia. [2, 125, 126]

Similarly to thermoradiosensitization, mild hyperthermia may also enhance the efficacy of cytotoxic antineoplastic drugs (thermochemosensitization). [75] Several chemotherapeutic agents have been shown to provide synergistic benefits with mild hyperthermia. These agents include cisplatin, melphalan, cyclophosphamide, nitrogen mustards, anthracyclines, nitrosoureas, blyeomycin, mitomycin C, and hypoxic cell sensitizers. [3, 75] Mechanisms for this synergistic behavior may include increased cellular uptake, increased oxygen radical production, as well as increased DNA damage and inhibition of repair. [3, 5, 98, 99] Furthermore, hypoxia and tissue acidity (pH) may also significantly affect the thermochemotherapeutic response, [127-129] as these adverse aspects of the tumor microenvironment are thought to be prevalent in areas of inadequate or inefficient vascular supply and may signify poor drug delivery. [130, 131] In contrary to hyperthermic radiotherapy, however, only few comparative trials have been completed to date where hyperthermia was applied as an adjunct to chemotherapy. [132-134]

2.5 Mild hyperthermia mediated drug and contrast agent delivery

Conventional chemotherapy usually relies on systemic drug delivery with limited specificity for tumor tissue, and therefore may result in dose-limiting toxicity, adverse side effects, and in reduced therapeutic efficacy. This scenario may be improved with the use of drug delivery systems (DDS) that selectively deliver chemotherapeutics to a tumor in an effort to reduce systemic toxicity and improve overall efficacy, consequently resulting in a larger therapeutic window. [10-12] DDS can be designed to improve both the pharmacological and therapeutic properties of certain drugs. A number of DDS have been developed, including micellic, liposomal, polymeric, biopolymeric, and monoclonal antibody-directed delivery. [12, 16-19] In particular, development of liposomes, which are artificially-prepared vesicles composed of a lipid bilayer, has resulted in a number of FDA-approved formulations for clinical use. [135] Encapsulation of a chemotherapeutic agent into liposomes may reduce systemic toxicity and enhance drug delivery compared with free drug. [12, 136, 137]

Liposomes can target the tumor either passively based on factors such as particle size and surface properties, or actively due to a specific affinity, activation, or stimulus. For example, passive tumor targeting can be achieved using stealth liposomes, which circulate and release their drug cargo over days or weeks and accumulate in tumor tissue through leaky tumor vasculature via the EPR effect. [14, 100, 101] Stealth liposomes have not been seen to penetrate deeply into tumor tissue, however, typically staying adjacent to blood vessels even two days after injection. [138] Moreover, slow drug release limits bioavailability even with long-circulating liposome accumulation into the tumor. [139] Despite these shortcomings, this passive targeting approach has been shown to produce 10-fold or greater drug delivery to a tumor over traditional chemotherapy. [140] Active tumor targeting can also be accomplished. For example, drug delivery can be achieved through incorporation of tumor-specific targeting ligands on the surface of the liposome, [141] as well as through liposomal components sensitive to stimuli such as pH, [142] electromagnetic radiation, [143] and enzymes. [144] In addition, tumors can be actively targeted by triggering intravascular release using temperature-sensitive liposomes (TSLs). [19, 20, 22, 145]

TSLs can be characterized by a gel-to-liquid crystalline phase transition temperature (T_t), which depends on the composition of the lipid bilayer membrane. [12, 19] At temperatures well below their T_t, TSLs are relatively stable. At or above T_t, the lipid bilayer becomes permeable and TSLs release their contents. TSLs with a T_t above human body temperature can therefore be used for local drug delivery if the target region is heated locally. [19, 24] These types of liposomes have recently gained considerable attention and have been used or are planned to be used in several clinical trials. [24, 146-149]

Contemporary TSLs are designed to release their cargo (usually a chemotherapy agent) at mild hyperthermic temperatures above a certain threshold temperature, typically around 40–41 °C. [19, 21, 25, 102] These kinds of liposomes, with release properties optimized for mild hyperthermia, are known as low-temperature sensitive liposomes (LTSLs), and they rapidly release their drug cargo upon being heated to their threshold temperature. [21] Fast-releasing LTSLs are well suited for intra-vascular triggered release, as they can release their contents within the transit time (a few seconds) of the tumor vascular network. [150-152] Preclinical studies combining LTSLs with local mild hyperthermia have demonstrated a significant tumor volume reduction in mouse tumor models compared with conventional free drug or non-thermally sensitive liposomes. [21, 22, 26, 27] Fig. 2.1 depicts targeted drug delivery resulting from the combination of mild hyperthermia and LTSLs.

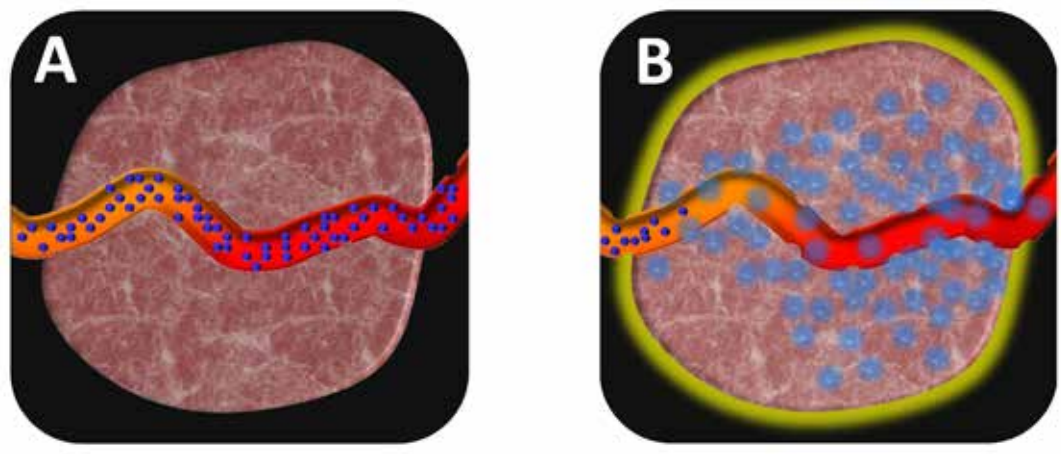

Fig. 2.1. Representation of mild hyperthermia mediated LTSL drug delivery. A) At normal body temperature, LTSLs (blue circles) circulate through tumor vasculature. B) At temperatures above the phase transition temperature of the lipid bilayer, LTSLs rapidly release their drug cargo resulting in targeted drug delivery to the tumor.

Although the efficacy of LTSLs has been studied in both preclinical and clinical settings, precise spatiotemporal control of drug delivery from LTSLs has not yet been achieved. [22, 24, 137, 146, 147] Intra- and inter-patient spatial variability in tumor microenvironment, such as vascularity and perfusion, may impact both the heating pattern and delivery of drugs. [28, 29, 153] To accommodate this spatial variability, mild hyperthermia treatment may be adjusted for optimal drug delivery by using a control algorithm. Therefore, in addition to temperature monitoring, direct imaging of drug delivery (or an appropriate substitute, such as release of a contrast agent from LTSL) may improve real-time control of drug delivery or help guide future interventions. A suitable surrogate for quantification of drug delivery may be provided by imaging contrast agent release from liposomes co-loaded with a drug and an MR contrast agent. [30]

Contrast agents can be used to improve the visibility of internal body structures in an MR image, as well as to study the transport properties of tissue by examining the dynamic changes in contrast enhancement. The first papers on liposomes loaded with MR contrast agents were published in the late 1980s. [154] These liposomes encapsulated high concentrations of hydrophilic contrast agents such as gadolinium-based Gd-DTPA. Recently, gadolinium-based contrast agents have been encapsulated in liposome interior compartment [31] as well as conjugated to their membrane, [32] or both. [33]

Relaxivity is an ability of magnetic compounds (e.g., contrast agents) to modify the relaxation rates of the surrounding water proton spins. Most liposomes with gadolinium-based contrast agents in their interior compartment have a relaxivity lower than that of free contrast agent, because their liposomal membrane shields contrast agent in the interior compartment from bulk water outside the liposome. [155] Such liposomes with contrast agents may be designed to report on drug delivery by contrast agent release. In fact, LTSLs that release contrast agent from their interior have been used to monitor release *in vivo*, demonstrating promising imaging correlations with both drug delivery [34] and therapeutic efficacy. [30] This ability may enable spatiotemporal control over drug delivery — a concept known as drug dose painting. [30, 34] In this paradigm, the treating physician prescribes a desired drug dose and spatial distribution of drug to be delivered, and an image-guided mild hyperthermia applicator manipulates heat in the target region to achieve the desired drug dose. Fig. 2.2 illustrates the use of imageable-LTSLs (iLTSLs) and an MR-HIFU system for drug dose painting.

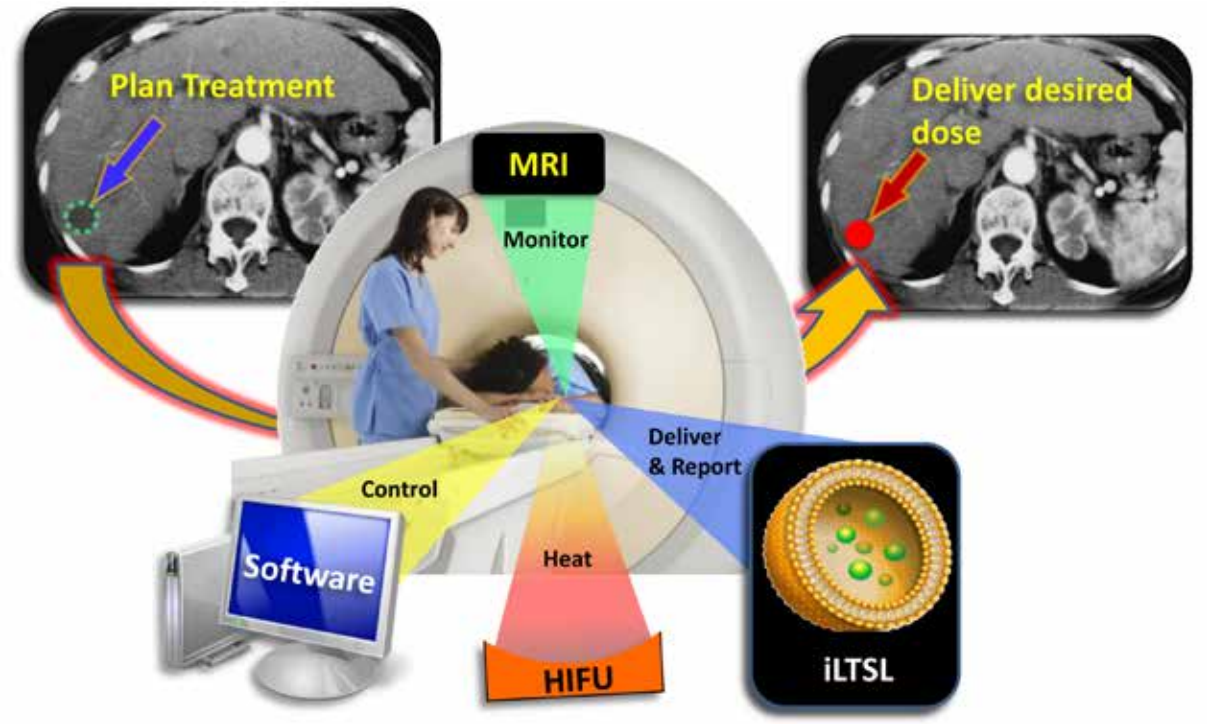

Fig. 2.2. A diagram showing the concept of drug dose painting using MR-HIFU and iLTSLs. The treating physician would select the area to deliver drug (green dashed circle), and the desired drug dose would be delivered preferentially to that region while the patient would be spared from the effects of systemic toxicity. A combination of MR imaging, HIFU heating, software-based automated feedback control, and iLTSLs would be used to plan, monitor, and control the treatment in real time.

3 High-intensity focused ultrasound

3.1 High-intensity focused ultrasound physics

3.1.1 Therapeutic ultrasound and high-intensity focused ultrasound

Acoustic waves are propagating pressure variations in a medium. Ultrasound is defined as a pressure wave that propagates at a frequency above 20 kHz, the typical threshold for human hearing. This longitudinal wave causes particles to oscillate back and forth and produce a series of compressions and rarefactions. Ultrasound waves deposit energy as they propagate through tissue, but the energy deposited by diagnostic ultrasound is insignificant, only slightly increasing tissue temperature ($\Delta T < 1.5$ °C). [156] It is to be noted that ultrasound will not readily penetrate air filled structures and thus cannot be used for imaging of, e.g., lung or bowel. [157]

Therapeutic ultrasound is a branch in medicine where living tissues are exposed to ultrasound waves with the intention of achieving beneficial results for health. Therapeutic applications of ultrasound predate its use as a diagnostic imaging technique. In 1927, Wood and Loomis recognized that ultrasound could produce lasting changes in biological systems, and initiated both safety and preclinical studies on ultrasound therapy. [158]

Therapeutic ultrasound operates according to the same physical principles as diagnostic ultrasound, although the total amount of deposited energy can be several orders of magnitude greater. Therapeutic ultrasound may be continuously applied for several seconds or even minutes. In contrast, diagnostic ultrasound is applied in short pulses of a few microseconds. The resulting spatial-peak temporal-average intensity levels (I_{spta}), indicative of the magnitude of thermal bioeffects, [159] are thus around 0.1–0.5 W/cm^2 for diagnostic ultrasound, even though the spatial-peak temporal-peak intensities (I_{sptp}) can be similar as for continuously applied therapeutic ultrasound. [43, 49, 60, 160] Typically, the spatial peak intensity levels for modern ultrasound therapy devices are around 1000–4660 W/cm^2 *in situ*, but can be significantly higher. [44, 49, 161, 162] Consequently, the increase in effective focal point intensity with focused therapeutic ultrasound can easily be a factor of 1000 or more, as compared to non-focused plane waves in diagnostic use. Therapeutic ultrasound modalities include, e.g., histotripsy, [163] lithotripsy, [164] ultrasound-enhanced thrombolysis, [165] and HIFU.

The properties of HIFU allow it to be brought into a tight focus at a distance from its source, with high, localized pressures leading to temperature elevations achieved solely within the focal region. [49, 160] The region or volume of elevated temperatures occurs without damage to surrounding tissues and can be targeted from outside the body, thus providing a noninvasive means to achieve hyperthermia (Fig. 3.1). A thorough overview of the fundamental principles of therapeutic ultrasound can be found in the *MRI-guided Focused Ultrasound Surgery* book compiled by Jolesz and Hynynen. [166]

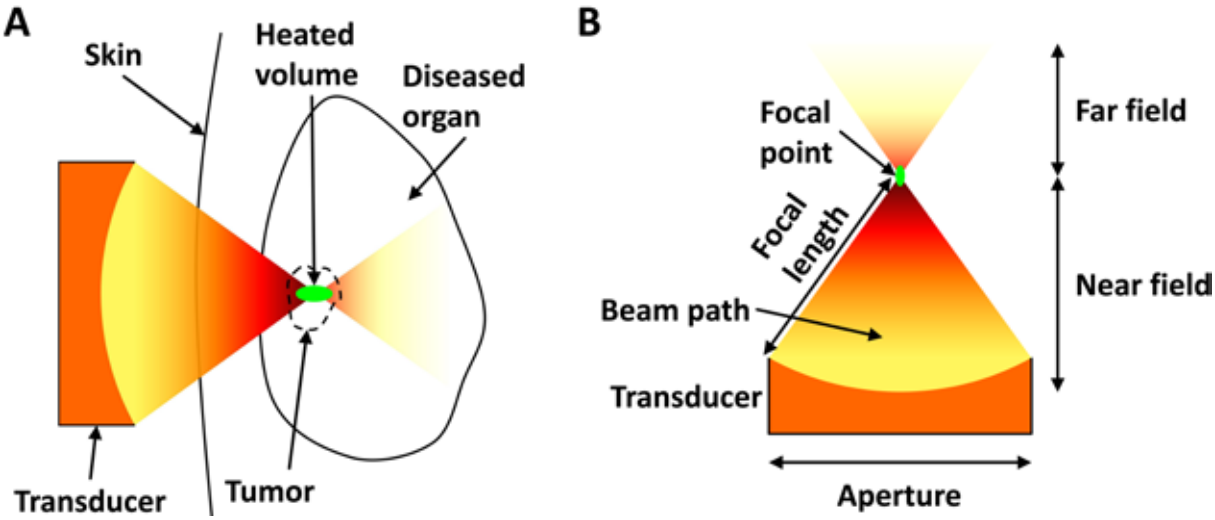

Fig. 3.1. A) Schematic representation of high-intensity focused ultrasound producing localized, elevated temperatures deep within the body, without significantly heating surrounding tissues. B) Schematic representation of a geometrically-focused spherical shell ultrasound transducer, showing near field, far field, beam path, aperture diameter, focal length, and the location of the focal point at the geometrical center of curvature. Depiction of the transducer, HIFU beam propagation, and the focal point are only illustrative and not to scale.

3.1.2 HIFU transducer design

Contemporary, clinical HIFU transducers are usually made of a piezoceramic or piezocomposite material, and come in the shape of a spherical shell. [50, 52, 55, 74, 167-170] A schematic representation of a geometrically focused spherical shell transducer is illustrated in Fig. 3.1. This kind of transducer has a natural focus at or near its geometric center of curvature, and provides much higher focal intensity gain compared to a non-focused planar transducer with similar dimensions. These features are especially useful for deep penetration and heat localization. [74, 168]

The resulting focal point is ellipsoid in shape, the size of which depends on transducer geometry and dimensions as well as on the ultrasound wavelength, but is typically in the order of few millimeters as measured at -3 dB or -6 dB of acoustic pressure. [169, 171] The wavelength λ, i.e., the distance between two compressions or rarefactions, is determined by the ultrasound frequency f according to [172]

$$\lambda = \frac{c}{f} \tag{3.1}$$

where c is the speed of sound in the attenuating medium. The speed of sound in human soft tissues is usually very close to that of water, i.e., approximately 1540 m/s. [173-175] In practice, extracorporeal HIFU transducers employ frequencies in the range of 0.6–2.0 MHz, whereas interstitial and intracavitary transducers use higher frequencies in the range of 2–6 MHz. [50, 55, 60, 61, 162, 171, 176-178]

For a typical HIFU transducer in clinical use, such as the one used in this dissertation work (Publications **I**–**VI**) with 256 elements, 12 cm radius of curvature (focal length), 13 cm aperture diameter, and operating at 1.2 MHz, the produced ellipsoid focal point is approximately 1.6 mm × 1.6 mm × 10 mm (-6 dB), as measured along the ellipsoid axes.

3.1.3 Phased arrays and electronic focal point deflection

In ultrasound wave theory, a phased array is an array of transducers in which the relative phases of the respective driving signals can be adjusted so that the effective wave pattern of the array is reinforced in desired locations (constructive interference) and suppressed in undesired locations (destructive interference).

A phased array HIFU transducer may consist of many small piezoelements, each of which can be individually controlled. [51,74,168,179-182] By adjusting the phase and/or amplitude of the driving radiofrequency signal individually for each element, the focal point can be displaced from the nominal focus, or a pattern of multiple foci can be generated. [51,77-79] In other words, the ultrasound beam can be steered or deflected electronically. This approach can be highly advantageous as it allows the heating of a larger volume as well as control of the shape of the heated volume without the need for mechanical displacement of the transducer, thus increasing both the flexibility and efficiency of a HIFU therapy. Fig. 3.2 demonstrates electronic steering of a single focal point using a phased-array transducer.

To obtain constructive interference at the desired location by electronic steering, the required phase for a given drive signal can be determined using the equation

$$\varphi_j = 2\pi \frac{l_j}{\lambda} \tag{3.2}$$

where $l_j = \left|\bar{r} - \bar{r}_j\right|$ denotes the distance from the center of the element $\bar{r}_j$ to the target focal point location $\bar{r}$ (Fig. 3.2).

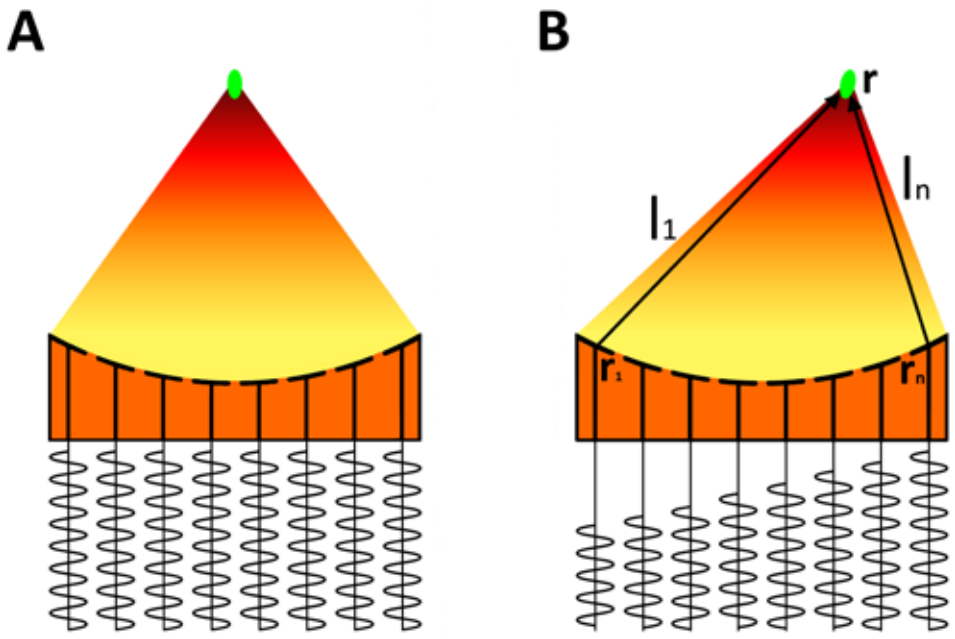

Fig. 3.2. Schematic illustration of a phased-array transducer, showing sinusoidal driving signals for each element. A) All elements are driven synchronously in phase, producing a focal point at the geometrical focus. B) By adjusting the relative phases of the drive signals, the focal point is displaced laterally (i.e., steered electronically). The l_1 and l_n denote the distances from the center of elements 1 (r_1) and n (r_n), respectively, to the target focal point location r.

The transducer design, i.e., its geometry and the number, location and size of the individual elements ultimately determine the volume within which the focal point can be steered, since the focal point has to be within the volume where all of the beams generated by the individual elements are overlapping. [166] If the focal point is steered outside of this volume, it results in loss of intensity at the intended focus, leading to inferior temperature elevation. Furthermore, it can lead to the generation of undesirable secondary focal points also known as side lobes, which usually occur in the opposite direction of deflection when steering the focal point laterally, perpendicular to the beam axis. [166] Element diameter in clinical phased-array HIFU transducers is typically around 2–10 mm, and thus they behave like directional radiation sources (element diameter > wavelength). Accordingly, electronic steering range is usually limited to approximately ±10–15 mm perpendicularly to the beam axis, and ±20 mm along the beam axis. [51, 169, 179]

The design of the phased-array transducer greatly influences the extent and severity of the side lobes. [169, 179] A symmetrically sectioned transducer surface with sizeable grating slits (i.e., areas that do not emit ultrasound) may result in moderate side lobes even without electronic steering, especially for transducers with a high degree of surface symmetry. Moreover, using these symmetrically designed transducers to perform electronic steering perpendicular to the beam axis may further escalate this problem. To remedy this, the symmetry of the element placement can be decreased by, e.g., utilizing a quasi-random design, thus reducing the extent of the side lobes and allowing for improved beam-steering. [74, 168, 183, 184] For manufacturing reasons, however, most transducers have some areas (between the elements) that do not emit ultrasound, resulting in minor side lobes that may or may not be insignificant, depending on the application.

3.2 HIFU platform

Due to a high characteristic acoustic impedance mismatch between water and air, ultrasound waves cannot readily propagate between the two media and therefore require a clear acoustic path between the transducer and target tissue. For modern clinical MR-HIFU platforms, this is typically achieved by immersing the transducer in a degassed water tank sealed with a very thin (50–100 µm) and acoustically transparent plastic membrane. [50, 55, 71, 170] The water tank is usually integrated into an MR-compatible patient table that also houses the matching electronics as well as an electromechanical transducer positioning system to enable accurate targeting. To assure and further improve acoustic coupling between the plastic membrane and the patient's skin, a gel pad together with ultrasound gel can be used. [50, 52] The MR-HIFU patient table is commonly incorporated into a freely movable unit that can be docked to the MR scanner for MR-HIFU therapy, and stowed away between procedures.

A clinical MR-HIFU therapy system (Sonalleve V1, Philips Healthcare, Vantaa, Finland) was utilized in this dissertation work for publications **I–VI**. This system consists of a patient table that houses the transducer as well as the positioning system. In addition, the system includes radiofrequency generators and amplifiers, control and matching electronics, MR receive coil, and a PC workstation with clinical software.

A clinical HIFU table may not be well suited for small animal studies, however, and might need an adapter for optimal coupling and animal positioning. An example of such adapter that contains an additional unsealed water bath located above the patient table, as well as a dedicated MR receive coil better suited for animal studies, is depicted in publication **II**.

3.3 Interaction of high-intensity focused ultrasound with tissue

3.3.1 Physical effects and mechanism of therapeutic action

Acoustic energy in tissue expresses itself as vibrational forces that are applied on every tissue component, such as intra- and extracellular fluids and cell membranes. An ultrasound wave propagating through the body may experience multiple and complex physical interactions between the wave and tissue that are capable of causing loss or redirection of acoustic energy. These interactions include reflection and refraction due to acoustic impedance mismatch between tissues, diffraction along inhomogeneous tissue, scattering, and absorption. Among these physical phenomena, scattering and absorption are thought to contribute the most to acoustic energy attenuation. As ultrasound energy is absorbed, it is converted to heat. When ultrasound is scattered due to tissue inhomogeneities, it is eventually absorbed elsewhere. [166, 185, 186] A detailed explanation on the interaction of ultrasound with biological tissues as well as of the principles of therapeutic ultrasound can be found in the *Physical Principles of Medical Ultrasonics* book compiled by Hill, Bamber, and ter Haar. [43]

HIFU bioeffects can be grouped into effects that are predominantly thermal or predominantly non-thermal (known as mechanical) in origin, and can be manipulated by adjusting ultrasound output power, frequency, duty cycle, sonication duration, and focal point characteristics. Non-thermal mechanisms can further be separated into cavitational and non-cavitational (not bubble-related) mechanisms. Thermal effects are due to ultrasound absorption and conversion to heat through vibrational excitation of tissue, leading to frictional heating and rapid, highly localized temperature elevation. Mechanical bioeffects include acoustic radiation forces and acoustic cavitation, which is mediated by bubble activity. Bubbles produced by cavitation are formed due to high negative peak pressures during the rarefaction phase of the ultrasound wave, and have been observed to prevent delivery of desired energy levels to the target region. In addition, collapsing or oscillating bubbles may lead to locally induced mechanical damage and enhanced heat absorption. [42, 186-188]

In the absence of blood flow, the rate of heating is determined by the attenuation coefficient, which is related to the density of the tissue and the ultrasound frequency. [166, 189] In the therapeutic ultrasound frequency range of interest, the relationship between ultrasound frequency and attenuation is approximately linear, i.e., higher frequencies cause an increase in attenuation. [43, 166] Ultrasound attenuation varies significantly between soft tissues, however, with a typical range of 0.3–2.0 dB/(cm·MHz), depending on tissue type. Attenuation for biological fluids can be much lower at around 0.1 dB/(cm·MHz), and much higher for bone at around 20 dB/(cm·MHz). [43, 173, 175]

The effects of HIFU on tissue are dependent on the acoustic pressure in the focal region, with different mechanisms of energy propagation dominating at different acoustic pressures. At low pressures, the acoustic field is predominantly linear and acoustic intensity is proportional to the pressure squared. At higher pressure levels, the peak negative (rarefaction) pressure correlates well with the onset of cavitation effects, [44, 190, 191] and nonlinear wave propagation leads to generation of higher harmonics. [192] Assuming linear acoustics in which the medium density and acoustic pressure have linear relationship, the pressure amplitude $p(x)$ of a propagating ultrasound wave is attenuated according to equation [172]

$$p(x) = p_0 e^{-\alpha x} \tag{3.3}$$

where x is the tissue depth, p_0 is pressure at $x = 0$, and α is the attenuation coefficient, which is the sum of the absorption and scattering coefficients α_a and α_s.

At the typical pressure levels produced by HIFU, however, the ultrasound propagation may be non-linear. The higher harmonic components of the fundamental frequency generated by the non-linearity are absorbed more rapidly, and thus may significantly increase local energy absorption especially in the focal region, thereby increasing the heating rate. [193-195]

3.3.2 Temperature rise induced by HIFU

The tissue temperature distribution $T(\bar{r},t)$ caused by energy absorption is often described using the Pennes' Bioheat Transfer Equation (BHTE) that takes into account heat diffusion as well as heat loss by perfusion. HIFU induced temperature rise as estimated by BHTE can be given by [196]

$$\rho_t c_t \frac{\partial T(\bar{r},t)}{\partial t} = \nabla \cdot \left(k_t \nabla T(\bar{r},t)\right) - w_{bl} c_{bl} \rho_{bl} \left(T(\bar{r},t) - T_{bl}\right) + Q(\bar{r},t) \tag{3.4}$$

where c_t is the specific heat of the tissue, ρ_t is the density of the tissue, k_t is the thermal conductivity of tissue, c_{bl} is the specific heat of blood, ρ_{bl} is the density of blood, w_{bl} is the blood perfusion rate, T_{bl} is the arterial blood temperature, and $Q(\bar{r},t)$ is the HIFU heat source term.

The energy absorption in tissue can be modeled as a function of the acoustic pressure amplitude p by [172]

$$Q(\bar{r},t) = \alpha \frac{p(\bar{r},t)^2}{\rho_t c} \tag{3.5}$$

where α is the attenuation coefficient, and c is the speed of sound in the tissue.

Since peak acoustic intensity I as a function of acoustic pressure for a plane progressive wave is [172]

$$I(\bar{r}) = \frac{p(\bar{r})^2}{\rho_t c} \tag{3.6}$$

the BHTE can be written using the product of acoustic intensity and attenuation as the heat source term

$$\rho_t c_t \frac{\partial T(\bar{r},t)}{\partial t} = \nabla \cdot \left(k_t \nabla T(\bar{r},t)\right) - w_{bl} c_{bl} \rho_{bl} \left(T(\bar{r},t) - T_{bl}\right) + \alpha I(\bar{r},t) \tag{3.7}$$

Speed of sound c in soft tissues varies slightly based on temperature, but is typically close to that in water, approximately 1540 m/s [173, 175]. Thermal conductivity k for most soft tissues is around 0.6 W/(m·°C), with the exception of fat. Fat is a relatively good insulator and consequently has a thermal conductivity around 0.2 W/(m·°C). [175, 197] In addition to constants α, c, and k_t being tissue dependent, however, physiological processes such as thermal coagulation change the properties of the heated tissue. [198] Furthermore, perfusion reduces the heating efficiency, and this effect can be significant in highly perfused organs such as kidney and liver, as well as in soft tissue tumors. [199-202] Thus, ultrasonic properties of tissue vary both in place and in time, and the exact temperature distributions in the target tissue cannot be theoretically calculated. For this reason, it is important to monitor the HIFU induced temperature elevations in real time not only in the target region, but in surrounding tissues as well.

3.3.3 Thermal dose

As with any thermal therapy, accurate temperature monitoring and methodical dosimetry are required to accomplish a beneficial and verifiable treatment outcome. Parameters such as minimum or average temperature, as well as the tenth percentile of the temperature distribution (T_{90}) based on multipoint thermometry have often been used. To manage temperature variations and diverse heating durations between patients, temperature data have been converted to quantifiable thermal dose, defined, e.g., as cumulative equivalent minutes at 43 °C (CEM_{43}) at the minimum, average, or T_{90} temperature point to enable comparative analysis. [123, 203] Many mild hyperthermia clinical trials have shown a positive correlation between thermal dose and treatment outcome. [105, 123, 124]

The concept of CEM_{43} thermal dose as a function of temperature and time was developed to quantitatively describe the effect of temperature elevation on tissue, and is defined in terms of equivalent minutes at the reference temperature of 43 °C.

The thermal dose after heating for time *t* is defined as [203]

$$TD_{43}\left(\bar{r},t\right)=\int_0^t R^{43-T\left(\bar{r},\tau\right)}d\tau \tag{3.8}$$

where $TD_{43}\left(\bar{r},t\right)$ is the thermal dose in equivalent minutes at 43 °C, $T\left(\bar{r},\tau\right)$ is the tissue temperature, and *R* is a constant that equals 0.5 above 43 °C and 0.25 below 43 °C. [203] The threshold for coagulative necrosis is thought to be between 50–250 CEM_{43}, depending on the tissue type, [51, 204-207] while thermal dose values of 10–50 CEM_{43} have been shown to provide a therapeutic effect in mild hyperthermia treatments. [208, 209] Thermal dose threshold of 240 CEM_{43} is generally considered as a good descriptor for irreversible thermal damage in most tissue types, [51, 206, 210-212] and is thus used in Publication **VI** as an indicator for complete coagulative necrosis.

3.4 Sonication strategies for mild hyperthermia

Typical focal point size for a HIFU transducer in clinical use is on the order of a few millimeters. On the other hand, the size of the target region in mild hyperthermia therapy may be significantly larger than the size of the focal spot: up to several centimeters in diameter. Furthermore, it would be preferable to simultaneously heat the whole target volume of cancerous tissue and keep it at an elevated temperature for up to an hour. [3, 4] An often used strategy for HIFU thermal ablations is to sequentially sonicate a number of focal points one at a time until the desired volume is ablated. [55, 170, 211, 213-215] This point-by-point sonication method is inherently inefficient, however, since a large part of the thermal energy is lost via heat diffusion out of the small sonication volume without being utilized for heating the target volume. Furthermore, this approach requires long treatment times since a large number of single point sonications are typically needed to cover the whole target volume, each separated by a cooling period to allow for transducer repositioning. Since mild hyperthermia therapy typically requires that the entire target lesion is heated for a long duration, the sequential point-by-point heating approach is not suitable for HIFU mediated mild hyperthermia. Clearly, other strategies for heating larger volumes to mild hyperthermic temperatures are required.

One such strategy is to move the transducer during a sonication to simultaneously heat a larger region by mechanically scanning the focal point within the target volume. [81, 137, 216-218] This sonication method tends to be relatively slow, however, and therefore is not well suited for maintaining large volumes at the target temperature range. [81, 218] In addition, this method may also be problematic to implement together with MR-imaging guidance, since a moving object with a substantially different magnetic susceptibility than its surroundings (i.e., an air-filled transducer in a liquid-filled tank) may cause perturbations in the magnetic field and ultimately lead to artifacts in the temperature images. [23, 219]

An alternative to mechanical transducer displacement is to utilize the electronic beam steering capabilities of a multielement phased array HIFU transducer. In this strategy, the focal point is rapidly steered along a single trajectory or multiple trajectories that can either be predetermined, or calculated in real time based on the resulting temperature distribution. Multiple locations can also be simultaneously sonicated by precisely adjusting the relative phases of the ultrasound driving signals and thus splitting the focus into multiple simultaneous foci. [78, 79, 168, 220] Furthermore, these multiple foci may be utilized for temporal switching between predetermined focal patterns while continuously sonicating. [77, 180, 221, 222] While multifoci sonication approaches have been described to cause side lobes in ablative hyperthermia, [74, 168, 182] these side lobes should not cause major problems in mild hyperthermia therapy due to the low acoustic pressures required by such treatments.

Sonication strategies of electronically sweeping a single focus point and simultaneously sonicating multiple concurrent foci may allow accurate and uniform mild hyperthermia in volumes much larger than a single focal point, while keeping the transducer stationary. These approaches for mild hyperthermia therapy were implemented on a clinical HIFU system, and tested and characterized in publications **I** and **II.** Furthermore, the single focus sweep strategy was employed in publications **III**, **IV**, and **V** for characterization of MR-HIFU mild hyperthermia mediated drug delivery.

The volumetric sonication approaches utilized in publications **I–VI** use the multiple outward-moving concentric circle trajectory concept originally proposed by Köhler et al. [51] In this concept, the circular trajectories are positioned in a plane perpendicular to the ultrasound beam axis and centered on the axis of propagation. Each circle contains multiple predetermined focal points that are evenly positioned on the circumference of the circle of a prescribed size. Examples of these circular trajectories are depicted in Fig. 3.3. In theory, however, these flexible volumetric sonication methods can utilize practically any trajectory shape, and may be designed and optimized according to patient- or application-specific requirements. While either mechanical transducer movement or electronic steering alone increase the volume that can be maintained at mild hyperthermia, the combination of these two methods may allow much larger volumes to be accurately heated.

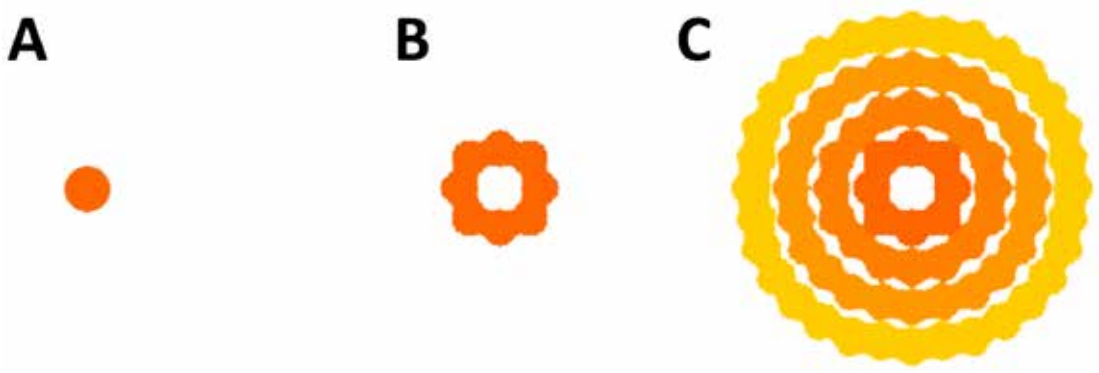

Fig. 3.3. Examples of circular sonication trajectories. A) 2 mm single sonication point. B) 4 mm circular sonication trajectory with 8 focal points. C) 16 mm circular sonication trajectory, which consists of four concentric subtrajectories: 4 mm circle (8 points), 8 mm circle (16 points), 12 mm circle (24 points), and 16 mm circle (32 points). In all trajectories, the focal points can be sonicated sequentially by electronically sweeping a single focus, or sonicated simultaneously by using multiple, concurrent foci.

3.5 Feedback controlled mild hyperthermia

Local, image-guided mild hyperthermia, especially in combination with temperature sensitive chemotherapeutics, is a clinically attractive and potentially feasible strategy for augmenting cancer therapies. For this strategy to realize its full potential, however, a hyperthermia applicator must be able to maintain accurate and homogenous heating in the cancerous target region while avoiding temperature rise in adjacent normal tissues.

With HIFU, the energy deposition and therefore the temperature increase and distribution depend on several tissue-specific parameters, such as ultrasound attenuation, heat diffusion, and tissue perfusion that are typically unknown. Therefore, it may be difficult to estimate the appropriate power level to achieve and maintain the desired narrow target temperature range. To overcome this problem, several feedback algorithms using real-time thermometry data have been proposed, with the objective of generating a spatiotemporally controlled temperature profile at the target region.

Feedback algorithms may allow for a fully controlled therapeutic procedure, ensuring that the correct amount of thermal energy is deposited at the targeted location while the adjacent, healthy tissues remain unheated. MR thermometry can be utilized to perform either operator adjustable or fully automated feedback control of HIFU therapy to improve the temperature accuracy and uniformity, as well as the overall treatment efficacy and safety. [88,96-100]

Current approaches for MR-HIFU feedback algorithms concentrate on the use of binary, proportional-integral (PI), or proportional-integral-derivative (PID) feedback control. [23, 72, 223-225] For example, feedback control methods in combination with spiral trajectories have been proposed for creating an accurate and uniform temperature elevation in the treatment volume. The acquired temperature data can be used to modify either the velocity of the focal point along the spiral trajectory, [81] or reoptimize the trajectory points after each spiral has been sonicated. [226] More advanced feedback methods have also been proposed, such as feedback control of the thermal dose and a 3D spatiotemporal temperature control scheme in a user-defined region of interest. [72, 227]

While these methods have been able to produce the desired thermal performance both *in vitro* and *in vivo*, most of these approaches are targeted for relatively short duration thermal ablations, [73, 80] or rely in part on *a priori* estimates of the energy absorption, heat diffusion, and local perfusion to prescribe an applied power. [81, 228] These tissue properties are known to be spatially heterogeneous and difficult or impossible to measure *in vivo*, potentially hindering the introduction of PI or PID feedback methods into clinical MR-HIFU mild hyperthermia workflow.

In publication **I**, a non-parametric binary mild hyperthermia feedback algorithm was designed and implemented on a clinical MR-HIFU system. This algorithm uses a temperature-based feedback approach that requires no prior knowledge of tissue-specific parameters, but instead monitors and responds to the actual measured temperature distribution in the target region. The control scheme can utilize multiple predetermined heating trajectories to produce and maintain accurate and homogeneous heating. Trajectory geometry and size, applied power, target temperature range, and therapy duration are set by the user. The trajectory shape and size can be arbitrary, and the feedback criteria can include minimum temperature, mean temperature, T_{90}, or thermal dose. The algorithm functions by comparing calculated temperatures to predetermined temperature limits, and switches the sonication trajectories accordingly. The simple design of this algorithm also provides robust control in the presence of disturbances, such as those related to sudden motion. Since the control scheme is based on sonication time while sonication power is limited in mild hyperthermia applications, there is no need for a smooth ramping to target temperature as is necessary for some parametric controllers, [23, 72, 82, 226] and thus rapid heat-up is possible. Comparative simplicity of the binary algorithm makes it an attractive candidate for clinical translation. Furthermore, regulatory implications may be more favorable for a simple and robust temperature feedback algorithm such as the one presented in publication **I**.

Despite the simplicity of concentric subtrajectories and binary control, the binary feedback algorithm presented in publication **I** does have some disadvantages. Since electronic steering can only be used to cover a relatively small volume, the binary approach cannot be used to heat much larger lesions commonly encountered in the clinic. In addition, the pre-defined subtrajectories used in the current binary implementation may not be adequate for heating spatially heterogeneous tissue, where dynamic changes in subtrajectory may be required for homogeneous heating. Even with these disadvantages, the binary feedback algorithm allowed for robust volumetric heating control, permitting examination of MR-HIFU mediated drug delivery in publications **III** and **V**.

4 Magnetic resonance guidance of high-intensity focused ultrasound mediated mild hyperthermia

4.1 Magnetic resonance imaging

Magnetic resonance imaging (MRI) is a noninvasive medical imaging technique used to produce detailed images of the body. The main advantage of MRI is that it does not rely on ionizing radiation to acquire images. Instead, MRI employs magnetic fields, magnetic field gradients, and radio frequency (RF) pulses. [229] MRI offers a variety of mechanisms to provide soft-tissue contrast, and it can highlight structural differences on both macroscopic and microscopic level in biological tissues. In addition, MRI can achieve excellent anatomical resolution and can be used to obtain images in any scan plane. [229] MRI is therefore well suited to depict and differentiate healthy and pathological tissues. As an added benefit, several MRI parameters are temperature sensitive, enabling noninvasive monitoring of temperature elevations during therapy by employing suitable MRI sequences. [48, 53] Consequently, MRI plays an important role in planning and monitoring surgical interventions and minimally invasive alternatives to surgery, such as HIFU. [46, 71, 166]

MRI exploits the physical properties of an atomic nucleus to induce measurable signals from the atoms of an object that is being imaged. The roots of MRI date back to 1938, when Isidor Rabi developed a new method for measuring the nuclear magnetic moment. [230] Later in 1946, Felix Bloch and Edward Purcell showed that the Nuclear Magnetic Resonance (NMR) phenomenon also exists in solid and liquid materials. [231, 232] The basis of the NMR effect is simply that nuclei in a magnetic field absorb and remit electromagnetic radiation at a specific resonance frequency (Larmor frequency) that depends on the strength of the magnetic field and the magnetic properties of the isotope of the atoms.

In the following sub-chapters, MRI-based therapy planning and monitoring, as well as MRI-based verification of therapy outcome are briefly discussed. A detailed explanation of NMR from the quantum point of view as well as descriptions of macroscopic magnetization, spin relaxation, and spatial encoding can be found in the excellent *Magnetic Resonance Imaging* book by Stark and Bradley. [229]

4.2 MRI-based therapy planning for mild hyperthermia therapy

MRI offers many advantages over other imaging techniques, such as ultrasound and computed tomography. Since MRI is devoid of ionizing radiation, it is of particular use in malignant tumor cases where repeated imaging may be necessary to monitor the progress of the disorder. Additional advantages include the ability to directly obtain images in multiple planes. Using contemporary clinical MR scanners, there is enough variation between intrinsic, tissue-specific MR parameters, such as T_1, T_2, or proton density, to permit image acquisition with excellent contrast between soft tissues, and between normal and abnormal morphology/pathology. [229] Furthermore, the effect of these tissue-specific parameters on the MR image contrast can be adjusted using a set of operator-selectable parameters, such as pulse repetition time (TR), echo time (TE), and flip angle (FA). [229] In addition, the use of an intravascular contrast agent (e.g., gadolinium chelates) may reveal physiologic changes in tissue that are associated with the underlying pathologies. Thus, in clinical practice, MRI is typically used for delineation of soft tissues, to determine extent and spread of disease, for staging of different tumors, to obtain functional and metabolic information, and for monitoring therapy response. [229]

The ability of MRI to display soft-tissue contrast and provide highly detailed images of the human body makes this noninvasive imaging modality also ideal for planning image-guided therapies, such as HIFU mediated mild hyperthermia. Treatment planning can be optimized by using software tools

and computer-assisted tissue delineation. For example, MR images can be shown within a graphical user interface and used in HIFU mild hyperthermia therapy planning to precisely define the treatment volume and HIFU beam path, as well as examine possible safety concerns, such as proximity of air filled cavities (e.g., lungs, bowel). This allows visualization and real-time adjustments of the therapy plan. Therapy planning may further be improved by superpositioning graphical overlays of, e.g., the transducer position, HIFU beam path, and target volume on the planning images. An example of HIFU mild hyperthermia therapy planning in an animal model is depicted in Fig. 4.1.

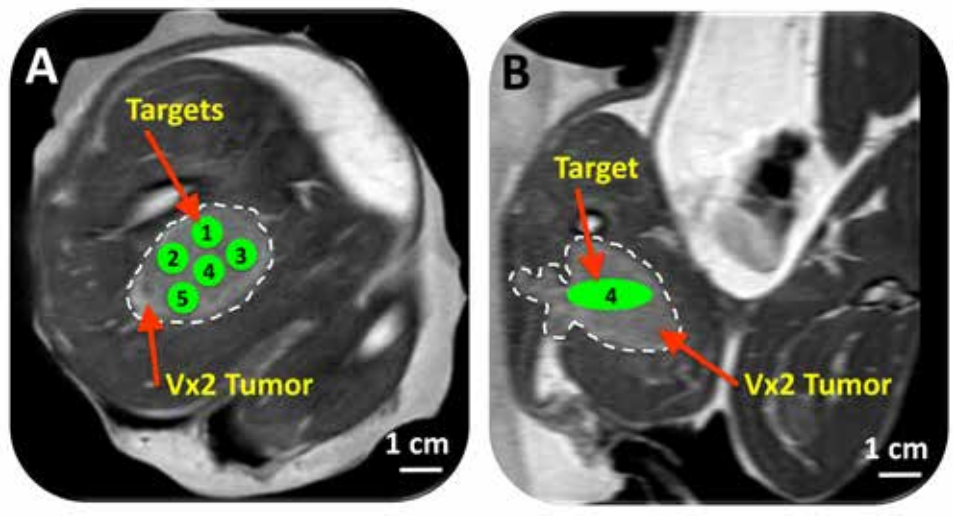

Fig. 4.1. Planning for MRI-guided mild hyperthermia: A) Coronal MR image, B) Sagittal MR image. Tumor (hyper-intense) was identified (white dashed line) on the proton density-weighted planning images, and target regions within the tumor were chosen (green circles). Image reproduced with slight modifications from Publication II with permission from AAPM.

4.3 Treatment monitoring by magnetic resonance thermometry

In mild hyperthermia therapy, the dependence of treatment success on achieved thermal dose highlights the requirement for precise temperature elevations and accurate thermal dosimetry. Invasive thermometry methods, such as insertion of thermocouples, suffer from poor sampling of just a few points in target tissue, with little to no sampling of surrounding tissues. [103, 187, 193, 233] In addition, this method is plagued by difficult placement and localization of the thermocouples, and may introduce imaging artifacts. [103] On the other hand, infrared cameras can detect temperature changes at submillimeter resolution, but *in vivo* measurements using this technique are limited to tissue surface. [234] The challenge of performing accurate thermal dosimetry has been one of the biggest hurdles in clinical mild hyperthermia therapy to date. [3]

At present, thermotherapies are monitored and guided by either ultrasound [233, 235, 236] or MRI. [48, 53, 57] Due to its availability, low cost, and easy application methods, ultrasound has been seen as the natural medium to direct HIFU therapy. Using the same medium as the thermotherapy itself would also seem sensible. The clear disadvantage of ultrasound is the relatively poor quality of images that can be difficult to interpret. In addition, ultrasound is incapable of concurrent treatment monitoring in multiple planes. Finally, despite promising experimental results, development of suitable ultrasound thermometry methods for real-time therapy monitoring in the clinic has been slow. [237] MRI currently offers the best solution for noninvasive assessment of temperature changes in tissue. [237] Several MR parameters are temperature sensitive, including diffusion coefficient, T_1 relaxation constant, bulk magnetization, and water proton resonance frequency. [48] The water proton resonance frequency shift (PRFS) method [47] has been shown to deliver the best temperature sensitivity, however, providing a temperature standard deviation of less than 1 °C at a temporal resolution below one second and a spatial resolution of roughly 2 mm. [53]

In addition, the PRFS method is nearly independent of tissue type and has excellent linearity of temperature dependency in non-adipose tissues. [48, 53] Thus, the PRFS method is currently the most commonly used for MR thermometry. [48] The PRFS of adipose tissue is not linearly dependent of temperature, however, and therefore fat suppression techniques are required in most biological tissues. [238, 239] PRFS-based MR thermometry was used in Publications **I–VI**, and its principles as well as its limitations are described below. Details on other MR thermometry techniques can be found in the review papers by Quesson et al. [53] and Denis de Senneville et al. [48]

4.3.1 Proton resonance frequency shift thermometry

Hindman first discovered PRFS's dependency on temperature in 1966, [240] when observing intramolecular forces and hydrogen bond formation between water molecules. Shielding by the surrounding molecules and electrons results in local variations in the B_0 main magnetic field experienced by individual protons. In water, the shielding is due to electrons of the hydrogen atoms. The electron cloud shields a hydrogen nucleus from the main magnetic field more efficiently when the nucleus is part of a free water molecule, as compared to a water molecule that is hydrogen bonded to another water molecule. This is because the hydrogen bonds distort the electronic configuration of the water molecules, thereby reducing the electronic shielding. The fraction of hydrogen bonded water molecules depends on the temperature. As temperature increases, the instability of hydrogen bonds also increases, and the molecules spend less time in a hydrogen-bonded state. [240, 241] This increases molecular shielding $\sigma(T)$ seen by the hydrogen nuclei and makes the local magnetic field B_{loc} experienced by nuclei temperature dependent according to equation [242]

$$B_{\text{loc}} = \left(1-\sigma\left(T\right)\right)B_0 = \left(1+\delta\left(T\right)\right)B_0 \tag{4.1}$$

where $\delta(T)$ is the resulting small difference in the proton resonance frequency, and is referred to as the chemical shift. Consequently, the proton resonance frequency also depends on temperature, and can be expressed as [242]

$$f = f_0\left(1+\delta\left(T\right)\right) \tag{4.2}$$

where f_0 is the Larmor frequency.

The chemical shift, which is reduced by the increase in molecular shielding, has almost linear temperature dependence that can be given as [242]

$$\delta\left(T\right) = \delta_0 + \alpha_T T \tag{4.3}$$

where δ_0 is the part of chemical shift that is independent of temperature, and α_T is the temperature dependency coefficient in ppm/°C. For water protons, α_T is -0.0108 ± 0.0001 ppm/°C. For soft tissue, α_T is typically between -0.009 and -0.01 ppm/°C, linearly dependent on the temperature within the temperature range of interest for hyperthermia, and nearly independent of tissue composition. [53, 240, 242, 243]

The decrease in the local magnetic field B_{loc} due to change in the temperature dependent chemical shift will also lower the proton resonance frequency that is linearly dependent on the local magnetic field. [231, 232] The temperature dependent shift in resonance frequency, and thus also the chemical shift, can be calculated from the phase maps generated, e.g., by gradient echo sequences, [47] as the signal phase Φ is directly proportional to the chemical shift according to [40, 41]

$$\Phi\left(T\right) = \gamma\delta\left(T\right)T_{\text{E}}B_0 \tag{4.4}$$

where γ is the gyromagnetic ratio and T_{E} is the echo time.

In order to measure only the temperature dependent change in the chemical shift, the temperature independent contribution δ_0 caused by B_0 field inhomogeneities must be removed. This is typically achieved by subtracting a reference phase map at a known baseline temperature from the phase map acquired at temperature T. Thus, the change in temperature can be calculated according to [48, 242]

$$\Delta T = \frac{\Phi(T) - \Phi(T_{\text{ref}})}{\gamma \alpha_T T_E B_0} \tag{4.5}$$

where $\Phi(T_{\text{ref}})$ is the corresponding reference phase at a known baseline temperature T_{ref}.

Accordingly, the PRFS technique is only capable of calculating relative temperature change, and not absolute temperatures. Therefore, the core body temperature is typically measured prior to therapy, and used as the baseline reference temperature T_{ref}, to which temperature change maps are added to obtain absolute temperature maps.

Using the PRFS method for thermometry at 1.5T field strength, with a TE of 20 ms, and with a signal-to-noise ratio (SNR) of 40, the theoretical temperature standard deviation can be as low as 0.3 °C. [81] Therefore, the PRFS method can achieve excellent temperature sensitivity.

An example of PRFS-based temperature monitoring during MR-HIFU mediated mild hyperthermia in an animal model is depicted in Fig. 4.2.

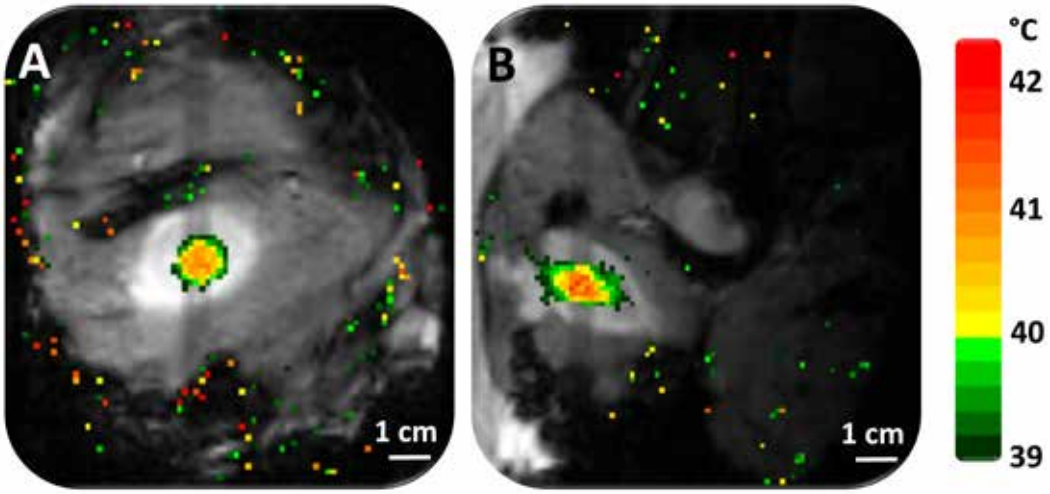

Fig. 4.2. PRFS-based temperature mapping for MR-HIFU mild hyperthermia: A) Coronal MR image, B) Sagittal MR image. Temperature maps (color scale) are overlaid on dynamic magnitude images (gray-scale), showing typical temperature distribution during HIFU heating. Target temperature range was 40.5–41 °C. Heating location corresponds to target region 4 in figure 4.1. Image reproduced from Publication II with permission from AAPM.

4.3.2 Complications of PRFS thermometry due to fatty tissues, motion, and magnetic field drift

The temperature dependence of PRFS in aqueous soft tissues has been shown to be nearly the same as in water. [48] In pure lipids, however, there are no hydrogen bonding interactions between molecules and thus the shielding constant does not vary significantly with temperature. [240] The PRFS of lipid hydrogen is therefore nearly independent of temperature, and the presence of even small amount of lipids in tissue may lead to significant errors in PRFS-based temperature maps. [238] To overcome this problem, fat suppression or spectrally selective excitation techniques can be applied to preferentially

image water protons, [244-246] thus allowing for accurate PRFS-based thermometry in tissues where both fat and water protons are present. [239] Regrettably, the fat signal cannot be completely suppressed due to the multiple resonance peaks present in fat (particularly the olefinic peak near water peak), and due to B_0 field inhomogeneities within the volume of interest.

Motion-related MR image artifacts occur when the imaged object moves during image acquisition. While registration and motion correction algorithms can be used to align the image with a reference image in order to correct for most bulk motion and avoid artifacts in the temperature images, there are motion-induced artifacts that cannot be corrected with registration. For example, B_0 field changes occur due to tissue motion, since the local magnetic field varies as the target tissue moves within the largely inhomogeneous magnetic field inside the body. Some of the most common motion-induced field changes occur due to breathing and cardiac motion, even at locations distant from the source of motion. These field changes may then result in phase changes in the images, which in turn cause temperature errors in PRFS-based MR thermometry. For example, breathing motion has been shown to induce field changes in the brain, [247, 248] abdomen, [249] and breast. [250, 251] Therefore, correct phase reference needs to be applied to enable accurate PRFS thermometry of or within close proximity of moving organs or objects. Many techniques have been developed to correct for these motion-induced phase changes and to provide a correct phase reference. Techniques include averaging or fitting of the MR data, but these methods typically require complex mathematical operations performed retrospectively, and may not be feasible for real-time use. [252, 253] In addition, navigator echoes for respiratory gating [254-256] as well as calculating differences in tissue position [257] have been used to estimate phase changes. Reference images taken at multiple stages of the breathing cycle (i.e., a multibaseline approach) can also be used in combination with respiratory gating to improve phase correction. [251, 258]

MR-HIFU mediated mild hyperthermia also poses a challenge not typically present in thermal ablation therapies in regards to MR thermometry. The duration of mild hyperthermia is usually much longer than that of an ablation, with typical treatment times in the order of tens of minutes and possibly as long as several hours. The B_0 magnetic field of modern MR scanners will drift over time when the gradients are intensely utilized. [259] This drift then causes non-temperature-related phase changes that are inseparable from temperature-related phase changes. Consequently, mild hyperthermia treatment durations allow for significant errors in temperature mapping. The exact amount of error on temperature depends on the type of magnet and gradient coils, performed calibrations, and the duration of therapy, but in modern well-calibrated systems can be in the order of 10 °C per hour. Taking into account that the intended temperature elevation for a typical hyperthermia treatment lies within 3–8 °C, field drift could pose a significant problem for temperature measurements if left uncorrected. Several methods have been developed to correct for the error arising from field drift. One common approach is to provide reference regions in the image that change phase with magnetic field drift but remain unheated, i.e., do not change phase with temperature. If the field drift varies spatially, an improved compensation can be achieved by fitting a polynomial curve to the spatial distribution of phase in the unheated reference region and subtracting this fitted phase from the acquired phase images. Other approaches include placing references (in thermal equilibrium) around the target and calculating the phase changes due to B_0 drift from these references. [238, 259] In addition, it has been shown that body fat or external water can be used as the reference material. [260]

Alternative PRFS-based methods for MR-HIFU include referenceless thermometry that is used to monitor phase change in surrounding unheated tissue and to extrapolate the phase correction into the heated tissue. This technique utilizes a polynomial fit of the phase [261, 262] or complex data [263] from the unheated area to estimate the background phase in the heated area. The background phase, i.e., the estimated phase in the heated area had it not been heated, is used as the phase reference. Thus, the effect of field drift is already included in the unheated area from which the reference phase is estimated, and a field drift correction is therefore not required. Disadvantages of this technique include the requirement for a relatively high SNR. In addition, the heating needs to be confined to a small well-defined area for the polynomial fit of the phase reference to be reliable, and thus this method may not be well suited for monitoring large volume MR-HIFU mild hyperthermia.

4.4 MRI verification of treatment outcome

While thermometry based thermal dose estimates have been used extensively as descriptors for assessing mild hyperthermia treatment outcomes, [105, 123, 124] other *in vivo* imaging methods are needed to quantify delivered drug, or to evaluate tissue damage resulting from ablative hyperthermia. The tissue effects of MR-HIFU mediated mild and ablative hyperthermia may result in changes in such MR tissue parameters as T_1 and T_2 relaxation constants, as well as in the magnetization transfer constant. [264-266] Thermally induced changes in tissue perfusion, diffusion, and stiffness may also be assessed using MRI. [265-270]

T_2-weighted imaging and contrast-enhanced imaging (CEI) are the two most commonly used MR-imaging methods to evaluate hyperthermia-induced tissue damage. The T_2 relaxation constant may change as a result of hyperthermia induced tissue damage. [264, 266] Consequently, T_2-weighted imaging can be used to locate the area of HIFU-induced thermal damage, [46, 57, 71, 264, 266] and previous studies have reported a good correlation between histological and T_2-weighted assessments of the thermal lesion size and shape post-therapy. [207, 271, 272] Similar comparisons between thermal dose and T_2-weighted assessment of the thermal lesion have also been described. [206, 207] T_2-weighted MRI is of limited use in assessing mild hyperthermia therapy, however.

On the other hand, CEI can be used to monitor MR-HIFU mediated drug delivery in combination with, e.g., imageable liposomes, as shown in publication **IV**. In addition, CEI can be utilized for evaluating the extent of coagulative necrosis post-treatment as exemplified in publication **VI**. The use of CEI to monitor iLTSL drug delivery as well as to assess therapy outcome of ablative HIFU is described below. Other imaging methods for verification of treatment outcome are also briefly discussed.

4.4.1 Contrast-enhanced MRI

MRI contrast agents alter the relaxation times of nuclei within tissues where they are present after administration. Most clinically used MRI contrast agents are administered intravenously, and function by shortening the T_1 relaxation time of nearby nuclei. In mild hyperthermia drug delivery utilizing iLTSL, CEI can be used to evaluate T_1-weighted signal intensity prior to and after imageable liposome injection, as well as to image contrast agent release in real-time or during and/or after each HIFU exposure. Direct imaging of delivered drug or an appropriate surrogate in the form of an MR contrast agent may improve real-time control of drug delivery or help guide and localize future interventions. [30] An example of the use of this technique is depicted in Fig. 4.3.

On the other hand, tissue vasculature may be necrotic within thermally coagulated tissue. [270-273] Consequently, the thermal lesions induced by ablative HIFU appear as hypointense (non-enhancing) regions in T_1-weighted CEI due to reduced contrast agent delivery to these non-perfused regions. [207, 256, 267, 270, 272] Good correlation has been shown between histological and CEI assessments of HIFU-induced regions of thermal coagulation. [206, 207, 256, 272] Because of this correlation to the gold standard of histology, CEI has been widely used in many MR-HIFU applications, including thermal ablation of symptomatic uterine leiomyomata. [52, 55, 274] The main drawback of CEI and the use of contrast agents is that the most commonly used compounds are gadolinium-based, which are non-toxic when chelated but may dechelate and release the highly toxic gadolinium ion if sufficiently heated. [275, 276] Currently, CEI in ablative hyperthermia is limited to post-therapy use for safety reasons.

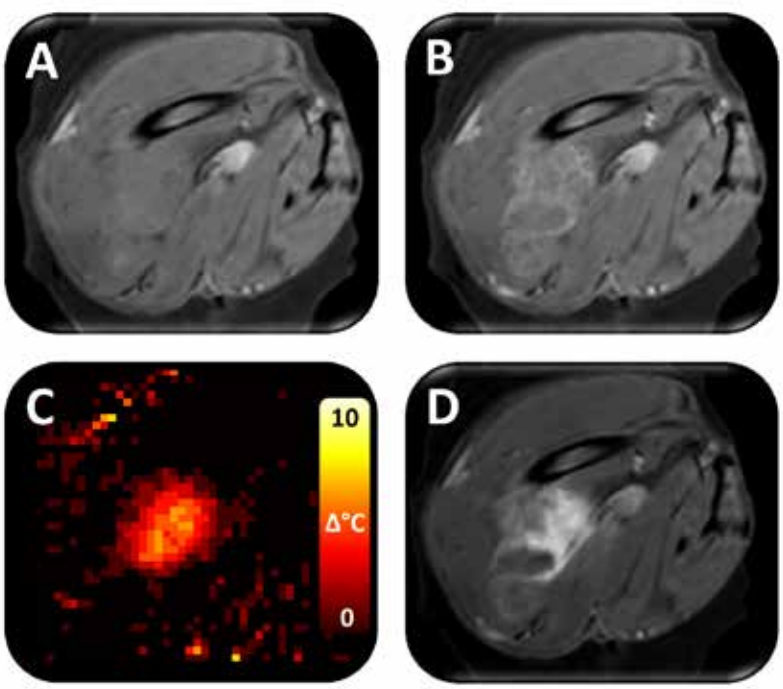

Fig. 4.3. MR signal intensity before and after iLTSL injection and heating with MR-HIFU. A) Signal intensity before iLTSL injection. B) Signal intensity after iLTSL injection. C) Example of a temperature elevation map during heating. D) Signal intensity after four 10-minute heating sessions. Preferential contrast agent release limited to the heated region is evident. A, B, and D depict T_1-weighted MR images.

4.4.2 Other MR-imaging methods for post-therapy assessment of efficacy

Diffusion MRI allows *in vivo* noninvasive mapping of water transport in biological tissues. Water transport in tissues is affected by tissue structure, and confined by macromolecules, fibers, and membranes, amongst others. Water molecule diffusion patterns can reveal details about normal and pathological tissue architecture. In diffusion-weighted imaging (DWI), each image voxel has a signal intensity that reflects a single best measurement of the local water transport rate. Consequently, DWI is sensitive to changes in the diffusion of water molecules in both the intra- and intercellular tissue environments, and can be used to assess immediate changes in the tissue structure post-therapy. [265, 277, 278]

DWI has been suggested for post-treatment prediction of HIFU-induced cell death, and its use to visualize necrotic tissue has been validated in previous studies. [265, 277-279] DWI may also be performed during therapy to assess therapy efficiency, unlike CEI that is limited to post-therapy use. In addition, it has been shown that the region of altered diffusion better correlates with the region of thermal damage than CEI-based assessment directly after HIFU therapy. [277] Disadvantages of DWI include high motion sensitivity, as well as long image acquisition times if high spatial resolution, information on directionality of transport, or multiple imaging slices are required. [277]

Finally, MR elastography can be used to produce images in which contrast is related to relative stiffness of tissue. By applying low frequency sound waves generated by an MRI-compatible acoustic driver, tissue stiffness or elasticity can be imaged by using special phase-contrast MR-imaging sequences. It has been previously reported that soft tissue elasticity may be reduced as a result of HIFU-induced thermal coagulation and protein denaturation, and that the subsequent reduction in elasticity can be assessed using MR elastography. [268, 280] Furthermore, PRFS-based MR thermometry can be performed using data acquired for MR elastography, thus allowing for simultaneous evaluation of tissue temperature and stiffness. [269] HIFU exposures also induce shear waves that can then be imaged with MR elastography, enabling concurrent production and assessment of MR-HIFU mediated thermal damage while estimating the temperature rise with PRFS thermometry. [269, 281, 282]

5 Discussion and conclusions

An optimal mild hyperthermia treatment would be spatially accurate, with precise and homogeneous heating limited to the target region while also limiting the likelihood of unwanted thermal or mechanical bioeffects. This places stringent requirements for both the hyperthermia applicator and the mild hyperthermia delivery methods. Feedback control of MR-HIFU mediated mild hyperthermia, based on the monitored temperature elevation, would be desirable for optimal therapy. Current approaches for MR-HIFU mild hyperthermia are limited in number, but focus on the use of PI or PID feedback control. [23, 72, 223-225] These methods rely in part on tissue parameters, such as local perfusion and ultrasound attenuation, which are largely unknown. In addition, these tissue properties are known to be spatially heterogeneous and difficult to measure *in vivo*, potentially hindering the introduction of proportional feedback controllers into clinical workflow. Publication **I** demonstrates the development and implementation of a binary mild hyperthermia feedback algorithm on a clinical MR-HIFU platform. Simplicity of the algorithm makes it an attractive candidate for clinical translation as a similar binary feedback method has already been applied in clinical MR-HIFU ablations. [50, 52]

The requirements placed upon mild hyperthermia heating strategies are very different compared to ablative hyperthermia. Desirable properties for ablation include high energy efficiency of the heating, as well as steep temperature gradients for improved lesion delineation. Consequently, steering a single high-intensity focus along circular trajectories in order to increase the ablation volume has shown benefit for ablation. [51, 52] On the other hand, heating uniformity is of much greater importance for mild hyperthermia, and high acoustic pressures resulting from the use of a single focal point may cause rapid, highly localized temperature elevations and unwanted mechanical bioeffects. Thus, operating at high acoustic pressures presents a potential problem in MR-HIFU mediated mild hyperthermia. Multifoci sonication patterns, which distribute the acoustic pressure over a larger area, possibly at the cost of slightly inferior heating efficiency and less well-defined treatment borders, may be beneficial for mild hyperthermia treatments. In addition, regulatory implications for MR-HIFU mediated mild hyperthermia may be more favorable for low acoustic pressures. Publication **II** presents the potential benefits of a multifoci sonication approach combined with a binary feedback algorithm for mild hyperthermia on a clinical MR-HIFU platform. Clinical oncology applications that require accurate and precise spatiotemporal control over heating (such as chemotherapeutic delivery and radiosensitization) may benefit from the improved safety and heating control offered by multifoci MR-HIFU mild hyperthermia.

LTSLs release their drug cargo in response to temperature elevations greater than the melting temperature of the lipid formulation. [19, 20] Studies combining LTSLs with local hyperthermia have demonstrated significant tumor volume reduction in mouse tumor models compared with conventional free drug or non-thermally sensitive liposome therapy. [21, 22, 26, 27] Furthermore, mild hyperthermia has been shown to assist drug delivery with liposomes by increasing the sensitivity of cancer cells to chemotherapeutics. [13] The combination of regionally targeted, image-guided mild hyperthermia and LTSLs is a clinically attractive and potentially feasible strategy for targeted delivery of drug to solid tumors. A variety of methods have been developed to achieve local, mild hyperthermia in a solid tumor for combination with LTSLs. [27, 283-285] Despite many technological advances, however, current hyperthermia applicators are often limited in their ability to provide a spatially accurate or deep thermal therapy to a solid tumor. To address these challenges, MR-HIFU may be combined with drug-containing LTSLs. The feasibility of combining MR-HIFU with clinical-grade LTSLs in a relevant Vx2 rabbit tumor model is demonstrated in publication **III**. This drug delivery technique may have potential for clinical translation as an image-guided method to deliver drug to a solid tumor.

Variability in tumor microenvironment may impact both the heating and delivery of drugs. [28, 29, 153] Direct imaging of drug delivery or an appropriate substitute may enable and improve real-time control of drug delivery. Co-loading cancer drug and MR contrast agent into LTSLs may provide a suitable substitute for quantifying drug delivery using MR-HIFU. LTSLs that release contrast agent from their interior have been used to monitor release *in vivo*, demonstrating correlation of imaging with drug delivery and therapeutic efficacy. [30, 34] Publication **IV** demonstrates the preparation and characterization of a novel

MR imageable liposome formulation (iLTSL) co-loaded with a cancer drug and an MR contrast agent. Monitoring of both heating and content release suggest that MR-HIFU mild hyperthermia combined with iLTSL may enable real-time spatial control of content release.

A variety of factors, including drug delivery system, drug characteristics, as well as physiological, biological, and biophysical parameters, affect hyperthermia-mediated drug delivery from LTSLs. Computer simulations provide a means to efficiently examine the effects of these parameters. In fact, *in silico* models have provided accurate descriptions of thermal therapies and drug delivery via LTSL and other carriers. [286, 287] In publication **V,** a mathematical model that combines a heat transfer model with a drug delivery model to simulate both HIFU-induced tissue heating and hyperthermia-mediated drug delivery was validated. The model can predict temperature distribution and delivered drug concentration and may thus allow quantitative comparison of different MR-HIFU heating algorithms as well as facilitate therapy planning for this drug delivery technique.

While the abovementioned materials and methods for MR-HIFU mediated mild hyperthermia and drug delivery are not yet available for clinical use, MR-HIFU technology is already being utilized in the clinic for the ablation of symptomatic uterine leiomyomata as well as for palliative treatment of painful osseous metastases. [50, 54-56, 62-64] For clinical translation of MR-HIFU mediated mild hyperthermia and drug delivery, it is important to show that current MR-HIFU therapy applications, using novel monitoring and control features, are safe and offer excellent spatial targeting accuracy as well as result in a predictable treatment outcome. In publication **VI**, a clinical MR-HIFU system was utilized for the treatment of symptomatic uterine leiomyomata in a phase I clinical trial. The novel safety and control features showcased in this publication may also facilitate the clinical acceptance of MR-HIFU mediated mild hyperthermia and drug delivery.

MR-HIFU mediated mild hyperthermia is an attractive option as a noninvasive hyperthermia therapy modality, especially in combination with drug delivery. The majority of the research for this dissertation was targeted at developing and validating materials and methods for safe, robust, and efficient MR-HIFU mediated mild hyperthermia and drug delivery for clinical use. The publications included in this dissertation serve as proof-of-principle and highlight the synergistic benefits that may be achieved using the combination of MR-imaging, HIFU, and LTSLs. However, for this technology to advance into the clinic and be used in cancer treatments on a routine basis, further developments may be required. These developments include large volume conformal MR-HIFU mediated mild hyperthermia, which may enable heating the whole tumor in a single therapy session. This method is currently under development. In addition, LTSLs can be designed to target cancerous tissue to further enhance drug delivery to tumor and reduce adverse side effects. [141] The concept of using MR-HIFU for clinically relevant mild hyperthermia and drug delivery is not just a far-fetched idea, but could very well be realized in the near future with some further improvements on the technology and methodology.

Fulfillment of the objectives

1. The developed MR-HIFU mild hyperthermia heating algorithm resulted in accurate and homogeneous heating within the targeted region in both tissue-mimicking phantoms and in a rabbit animal model. (**I**)

2. A multifoci sonication approach in combination with the mild hyperthermia heating algorithm resulted in accurate and precise heating within the targeted region with significantly lower acoustic pressures and spatially more confined heating, as compared to a single focus sonication method. (**II**)

3. LTSL + MR-HIFU resulted in significantly higher tumor drug concentrations compared to free drug and LTSL alone. This technique may have potential for clinical translation as a method to deliver drug to a solid tumor. (**III**)

4. MR-HIFU enabled monitoring of both heating and content release from a novel MR imageable liposome formulation co-loaded with drug and a contrast agent. (**IV**)

5. A computational model, which can predict temperature distribution and delivered drug concentration resulting from combining MR-HIFU with LTSLs, was validated in an *in vivo* study. (**V**)

In addition, a clinical MR-HIFU system was utilized in publication **VI** for the treatment of symptomatic uterine leiomyomata in a phase I clinical trial, showcasing that this therapy modality is feasible, safe, and already in clinical use with impressive targeting accuracy.

6 Summary of the publications

Publication I: A binary mild hyperthermia feedback algorithm was developed and implemented on a clinical MR-HIFU platform. Sonications resulted in accurate and homogeneous heating within the targeted region in both tissue-mimicking phantom and in a rabbit muscle and Vx2 tumor. Mean temperatures between 40.4 °C and 41.3 °C with a standard deviation of 1.0–1.5 °C (T_{10} = 41.7–43.7 °C, T_{90} = 39.0–39.6 °C) were measured *in vivo*, in agreement with *in vitro* studies. 3D spatial offset was 0.1–3.2 mm *in vitro* and 0.6–4.8 mm *in vivo*, demonstrating good spatial targeting accuracy. Combination of MR-HIFU mild hyperthermia and LTSLs demonstrated heterogeneous delivery to a partially heated Vx2 tumor.

Publication II: A multifoci sonication approach was combined with the mild hyperthermia heating algorithm developed in publication **I**, and implemented on a clinical MR-HIFU platform. According to both acoustic simulations and hydrophone measurements, the multifoci approach produced significantly lower (67% reduction) acoustic peak pressures in the focal region. Combined with the feedback algorithm, the multifoci heating method provided robust temperature control, resulting in accurate and precise heating within the targeted regions in a tissue-mimicking phantom, in normal rabbit muscle, and in a Vx2 tumor. The multifoci heating approach also resulted in better temperature uniformity in the target region and more confined heating in the beam path direction compared to the single focus sweep sonication method in both simulations and experiments.

Publication III: Clinical-grade LTSLs encapsulating doxorubicin were used with a clinical MR-HIFU platform to investigate *in vivo* image-guided drug delivery. Fifteen rabbits with Vx2 tumors within superficial thigh muscle were randomly assigned into three treatment groups of free doxorubicin, LTSL, and LTSL+MR-HIFU. Using a clinical MR-HIFU system and the heating algorithm developed in publication **I**, sonication of Vx2 tumors resulted in accurate (mean = 40.5±0.1 °C) and spatially homogenous (SD = 1.0 °C) temperature control in the target region. LTSL+MR-HIFU resulted in significantly higher tumor drug concentrations compared to free drug (7.6-fold increase) and LTSL alone (3.4-fold increase), despite heating only part of the tumor. Feasibility of combining MR-HIFU mediated mild hyperthermia with a clinical-grade LTSL in a relevant Vx2 rabbit tumor model was demonstrated.

Publication IV: A novel MR-imageable liposome formulation co-loaded with an MRI contrast agent and doxorubicin was developed, and its release at mild hyperthermic temperatures was characterized. Release with MR-HIFU was examined in tissue-mimicking phantoms and in a Vx2 rabbit tumor model. iLTSL demonstrated consistent size and doxorubicin release kinetics after storage at 4 °C for 7 days. Release of doxorubicin and contrast agent from iLTSL was minimal at 37 °C but fast when heated to over 41 °C. Relaxivity of iLTSL increased significantly (from 1.95±0.05 to 4.0±0.1 mMs^{-1}) when heated above the phase transition temperature. Signal increase corresponded spatially and temporally to MR-HIFU-heated locations both in phantoms and *in vivo*. MR-HIFU enabled monitoring of content release as well as control and monitoring of heating.

Publication V: A computational model that simulates MR-HIFU mediated heating of tissue as well as the resulting hyperthermia-mediated drug delivery from LTSLs was developed, and validated *in vivo* using a clinical MR-HIFU system and the heating algorithm developed in publication **I**. MR-HIFU heating in tissue was simulated using a heat transfer model based on the bioheat equation. A spatiotemporal multicompartment pharmacokinetic model simulated intravascular release of drug from LTSL, its transport into interstitium, and cell uptake. Mild hyperthermia produced a defined region of high drug concentration in the target region both *in silico* and *in vivo*. *In silico*, cellular drug uptake was directly related to hyperthermia duration, with increasing uptake up to 2 h. Within the heated region, temperature difference between the model and the experiment was on average 0.54 °C, and the doxorubicin concentration profile predicted by the model agreed qualitatively with the distribution of doxorubicin fluorescence *in vivo*.

Publication VI: A clinical MR-HIFU system was utilized for the treatment of symptomatic uterine leiomyomata in a phase I clinical trial, as a preliminary investigation into the safety and targeting accuracy of the treatment. Adverse events, imaging findings, targeting accuracy, and pathologic evidence of ablation were assessed. Eleven women underwent MR-HIFU ablation followed by hysterectomy within 30 days of treatment. No serious adverse events were observed, and histopathological assessment as well as MR imaging revealed that all leiomyomata were ablated in the planned location. No significant differences were observed in ablation volume size between MR imaging and histopathology. Mean misregistration values were 0.8±1.2 mm in feet-head direction, 0.1±1.0 mm in left-right direction, and 0.7±3.1 mm along the beam axis. Safe and accurate ablation of uterine leiomyomata was achieved using MR-HIFU.

References

1 M.D. Bert Vogelstein, B.V.K.W. Kinzler, *The Genetic Basis of Human Cancer*, 2nd ed. (McGraw-Hill, 2002).

2 *Holland Frei Cancer Medicine*, 8th ed. (People's Medical Publishing House-USA, Shelton, CT, 2010).

3 B.L. Viglianti, P. Stauffer, E. Repasky, E. Jones, Z. Vujaskovic, M.W. Dewhirst, "Hyperthermia," in *Holland Frei Cancer Medicine,* edited by H. W., B.R. Jr, H. W., K. D.W., H. J.F., P. R.E., e. al. (People's Medical Publishing House-USA, Shelton, CT, 2010), pp. 528-540.

4 R.D. Issels, L.H. Lindner, J. Verweij, P. Wust, P. Reichardt, B.C. Schem, S. Abdel-Rahman, S. Daugaard, C. Salat, C.M. Wendtner, Z. Vujaskovic, R. Wessalowski, K.W. Jauch, H.R. Durr, F. Ploner, A. Baur-Melnyk, U. Mansmann, W. Hiddemann, J.Y. Blay, P. Hohenberger, "Neo-adjuvant chemotherapy alone or with regional hyperthermia for localised high-risk soft-tissue sarcoma: a randomised phase 3 multicentre study," Lancet Oncol **11**, 561-570 (2010).

5 G.M. Hahn, *Hyperthermia and Cancer*. (Plenum Press, New York, 1982).

6 B.J. Wood, J.R. Ramkaransingh, T. Fojo, M.M. Walther, S.K. Libutti, "Percutaneous tumor ablation with radiofrequency," Cancer **94**, 443-451 (2002).

7 J. van der Zee, "Heating the patient: a promising approach?," Ann Oncol **13**, 1173-1184 (2002).

8 P. Wust, B. Hildebrandt, G. Sreenivasa, B. Rau, J. Gellermann, H. Riess, R. Felix, P.M. Schlag, "Hyperthermia in combined treatment of cancer," Lancet Oncol **3**, 487-497 (2002).

9 M.H. Falk, R.D. Issels, "Hyperthermia in oncology," Int J Hyperthermia **17**, 1-18 (2001).

10 Y.H. Bae, K. Park, "Targeted drug delivery to tumors: myths, reality and possibility," J Control Release **153**, 198-205 (2011).

11 T.M. Allen, P.R. Cullis, "Drug delivery systems: entering the mainstream," Science **303**, 1818-1822 (2004).

12 V.V. Ranade, J.B. Cannon, *Drug Delivery Systems*. (CRC Press, Boca Raton, 2011).

13 C.D. Landon, J.-Y. Park, D. Needham, M.W. Dewhirst, "Nanoscale Drug Delivery and Hyperthermia: The Materials Design and Preclinical and Clinical Testing of Low Temperature-Sensitive Liposomes Used in Combination with Mild Hyperthermia in the Treatment of Local Cancer," The Open Nanomedicine Journal **3**, 38-64 (2011).

14 G. Kong, R.D. Braun, M.W. Dewhirst, "Characterization of the effect of hyperthermia on nanoparticle extravasation from tumor vasculature," Cancer Res **61**, 3027-3032 (2001).

15 G. Kong, M.W. Dewhirst, "Hyperthermia and liposomes," Int J Hyperthermia **15**, 345-370 (1999).

16 W. Li, X. Cai, C. Kim, G. Sun, Y. Zhang, R. Deng, M. Yang, J. Chen, S. Achilefu, L.V. Wang, Y. Xia, "Gold nanocages covered with thermally-responsive polymers for controlled release by high-intensity focused ultrasound," Nanoscale **3**, 1724-1730 (2011).

17 M.R. Dreher, W. Liu, C.R. Michelich, M.W. Dewhirst, A. Chilkoti, "Thermal cycling enhances the accumulation of a temperature-sensitive biopolymer in solid tumors," Cancer Res **67**, 4418-4424 (2007).

18 J.S. Park, Y. Akiyama, Y. Yamasaki, K. Kataoka, "Preparation and characterization of polyion complex micelles with a novel thermosensitive poly(2-isopropyl-2-oxazoline) shell via the complexation of oppositely charged block ionomers," Langmuir **23**, 138-146 (2007).

19 M.B. Yatvin, J.N. Weinstein, W.H. Dennis, R. Blumenthal, "Design of liposomes for enhanced local release of drugs by hyperthermia," Science **202**, 1290-1293 (1978).

20 J.N. Weinstein, R.L. Magin, M.B. Yatvin, D.S. Zaharko, "Liposomes and local hyperthermia: selective delivery of methotrexate to heated tumors," Science **204**, 188-191 (1979).

21 G. Kong, G. Anyarambhatla, W.P. Petros, R.D. Braun, O.M. Colvin, D. Needham, M.W. Dewhirst, "Efficacy of liposomes and hyperthermia in a human tumor xenograft model: importance of triggered drug release," Cancer Res **60**, 6950-6957 (2000).

[22] D. Needham, G. Anyarambhatla, G. Kong, M.W. Dewhirst, "A new temperature-sensitive liposome for use with mild hyperthermia: characterization and testing in a human tumor xenograft model," Cancer Res **60**, 1197-1201 (2000).

[23] R. Staruch, R. Chopra, K. Hynynen, "Localised drug release using MRI-controlled focused ultrasound hyperthermia," Int J Hyperthermia **27**, 156-171 (2011).

[24] R.T. Poon, N. Borys, "Lyso-thermosensitive liposomal doxorubicin: a novel approach to enhance efficacy of thermal ablation of liver cancer," Expert Opin Pharmacother **10**, 333-343 (2009).

[25] D. Needham, M.W. Dewhirst, "The development and testing of a new temperature-sensitive drug delivery system for the treatment of solid tumors," Adv Drug Deliv Rev **53**, 285-305 (2001).

[26] T.P. Chelvi, S.K. Jain, R. Ralhan, "Hyperthermia-mediated targeted delivery of thermosensitive liposome-encapsulated melphalan in murine tumors," Oncol Res **7**, 393-398 (1995).

[27] P.S. Yarmolenko, Y. Zhao, C. Landon, I. Spasojevic, F. Yuan, D. Needham, B.L. Viglianti, M.W. Dewhirst, "Comparative effects of thermosensitive doxorubicin-containing liposomes and hyperthermia in human and murine tumours," Int J Hyperthermia **26**, 485-498 (2010).

[28] W. Schramm, D. Yang, D. Haemmerich, "Contribution of direct heating, thermal conduction and perfusion during radiofrequency and microwave ablation," Conf Proc IEEE Eng Med Biol Soc **1**, 5013-5016 (2006).

[29] A. Gasselhuber, M.R. Dreher, A. Negussie, B.J. Wood, F. Rattay, D. Haemmerich, "Mathematical spatio-temporal model of drug delivery from low temperature sensitive liposomes during radiofrequency tumour ablation," Int J Hyperthermia **26**, 499-513 (2010).

[30] A.M. Ponce, B.L. Viglianti, D. Yu, P.S. Yarmolenko, C.R. Michelich, J. Woo, M.B. Bally, M.W. Dewhirst, "Magnetic resonance imaging of temperature-sensitive liposome release: drug dose painting and antitumor effects," J Natl Cancer Inst **99**, 53-63 (2007).

[31] K. Ghaghada, C. Hawley, K. Kawaji, A. Annapragada, S. Mukundan, Jr., "T1 relaxivity of core-encapsulated gadolinium liposomal contrast agents--effect of liposome size and internal gadolinium concentration," Acad Radiol **15**, 1259-1263 (2008).

[32] S. Laurent, L.V. Elst, C. Thirifays, R.N. Muller, "Paramagnetic liposomes: inner versus outer membrane relaxivity of DPPC liposomes incorporating lipophilic gadolinium complexes," Langmuir **24**, 4347-4351 (2008).

[33] K.B. Ghaghada, M. Ravoori, D. Sabapathy, J. Bankson, V. Kundra, A. Annapragada, "New dual mode gadolinium nanoparticle contrast agent for magnetic resonance imaging," PLoS One **4**, e7628 (2009).

[34] B.L. Viglianti, S.A. Abraham, C.R. Michelich, P.S. Yarmolenko, J.R. MacFall, M.B. Bally, M.W. Dewhirst, "In vivo monitoring of tissue pharmacokinetics of liposome/drug using MRI: illustration of targeted delivery," Magn Reson Med **51**, 1153-1162 (2004).

[35] L. Wu, R.J. McGough, O.A. Arabe, T.V. Samulski, "An RF phased array applicator designed for hyperthermia breast cancer treatments," Phys Med Biol **51**, 1-20 (2006).

[36] D. Fatehi, J. van der Zee, M. de Bruijne, M. Franckena, G.C. van Rhoon, "RF-power and temperature data analysis of 444 patients with primary cervical cancer: deep hyperthermia using the Sigma-60 applicator is reproducible," Int J Hyperthermia **23**, 623-643 (2007).

[37] T. Juang, P.R. Stauffer, D.G. Neuman, J.L. Schlorff, "Multilayer conformal applicator for microwave heating and brachytherapy treatment of superficial tissue disease," Int J Hyperthermia **22**, 527-544 (2006).

[38] D.R. Boreham, H.C. Gasmann, R.E. Mitchel, "Water bath hyperthermia is a simple therapy for psoriasis and also stimulates skin tanning in response to sunlight," Int J Hyperthermia **11**, 745-754 (1995).

[39] R.J. McNichols, M. Kangasniemi, A. Gowda, J.A. Bankson, R.E. Price, J.D. Hazle, "Technical developments for cerebral thermal treatment: water-cooled diffusing laser fibre tips and temperature-sensitive MRI using intersecting image planes," Int J Hyperthermia **20**, 45-56 (2004).

[40] T.O. Tasci, I. Vargel, A. Arat, E. Guzel, P. Korkusuz, E. Atalar, "Focused RF hyperthermia using magnetic fluids," Medical Physics **36**, 1906-1912 (2009).

[41] A. Jordan, P. Wust, H. Fahling, W. John, A. Hinz, R. Felix, "Inductive heating of ferrimagnetic particles and magnetic fluids: physical evaluation of their potential for hyperthermia. 1993," Int J Hyperthermia **25**, 499-511 (2009).

[42] W.J. Fry, V.J. Wulff, D. Tucker, F.J. Fry, "Physical Factors Involved in Ultrasonically Induced Changes in Living Systems: I. Identification of Non-Temperature Effects," J Acoust Soc Am **22**, 867-876 (1950).

[43] C.R. Hill, J.C. Bamber, G.R. ter Haar, *Physical principles of medical ultrasonics.* , 2nd ed. (John Wiley & Sons Ltd, 2004).

[44] M. Bailey, V. Khokhlova, O. Sapozhnikov, S. Kargl, L. Crum, "Physical mechanisms of the therapeutic effect of ultrasound (a review)," Acoustical Physics **49**, 369-388 (2003).

[45] J.G. Lynn, R.L. Zwemer, A.J. Chick, A.E. Miller, "A New Method for the Generation and Use of Focused Ultrasound in Experimental Biology," J Gen Physiol **26**, 179-193 (1942).

[46] K. Hynynen, A. Darkazanli, E. Unger, J.F. Schenck, "MRI-guided noninvasive ultrasound surgery," Med Phys **20**, 107-115 (1993).

[47] Y. Ishihara, A. Calderon, H. Watanabe, K. Okamoto, Y. Suzuki, K. Kuroda, "A precise and fast temperature mapping using water proton chemical shift," Magn Reson Med **34**, 814-823 (1995).

[48] B. Denis de Senneville, B. Quesson, C.T. Moonen, "Magnetic resonance temperature imaging," Int J Hyperthermia **21**, 515-531 (2005).

[49] J.E. Kennedy, G.R. Ter Haar, D. Cranston, "High intensity focused ultrasound: surgery of the future?," Br J Radiol **76**, 590-599 (2003).

[50] M.J. Voogt, H. Trillaud, Y.S. Kim, W.P. Mali, J. Barkhausen, L.W. Bartels, R. Deckers, N. Frulio, H. Rhim, H.K. Lim, T. Eckey, H.J. Nieminen, C. Mougenot, B. Keserci, J. Soini, T. Vaara, M.O. Köhler, S. Sokka, M.A. van den Bosch, "Volumetric feedback ablation of uterine fibroids using magnetic resonance-guided high intensity focused ultrasound therapy," Eur Radiol **22**, 411-417 (2012).

[51] M.O. Köhler, C. Mougenot, B. Quesson, J. Enholm, B. Le Bail, C. Laurent, C.T. Moonen, G.J. Ehnholm, "Volumetric HIFU ablation under 3D guidance of rapid MRI thermometry," Med Phys **36**, 3521-3535 (2009).

[52] Y.S. Kim, B. Keserci, A. Partanen, H. Rhim, H.K. Lim, M.J. Park, M.O. Köhler, "Volumetric MR-HIFU ablation of uterine fibroids: Role of treatment cell size in the improvement of energy efficiency," Eur J Radiol **81**, 3652-3659 (2012).

[53] B. Quesson, J.A. de Zwart, C.T. Moonen, "Magnetic resonance temperature imaging for guidance of thermotherapy," J Magn Reson Imaging **12**, 525-533 (2000).

[54] E.A. Stewart, J. Rabinovici, C.M. Tempany, Y. Inbar, L. Regan, B. Gostout, G. Hesley, H.S. Kim, S. Hengst, W.M. Gedroyc, "Clinical outcomes of focused ultrasound surgery for the treatment of uterine fibroids," Fertil Steril **85**, 22-29 (2006).

[55] C.M. Tempany, E.A. Stewart, N. McDannold, B.J. Quade, F.A. Jolesz, K. Hynynen, "MR imaging-guided focused ultrasound surgery of uterine leiomyomas: a feasibility study," Radiology **226**, 897-905 (2003).

[56] Y.S. Kim, H. Trillaud, H. Rhim, H.K. Lim, W. Mali, M. Voogt, J. Barkhausen, T. Eckey, M.O. Köhler, B. Keserci, C. Mougenot, S.D. Sokka, J. Soini, H.J. Nieminen, "MR Thermometry Analysis of Sonication Accuracy and Safety Margin of Volumetric MR Imaging-guided High-Intensity Focused Ultrasound Ablation of Symptomatic Uterine Fibroids," Radiology **265**, 627-637 (2012).

[57] K. Hynynen, O. Pomeroy, D.N. Smith, P.E. Huber, N.J. McDannold, J. Kettenbach, J. Baum, S. Singer, F.A. Jolesz, "MR imaging-guided focused ultrasound surgery of fibroadenomas in the breast: a feasibility study," Radiology **219**, 176-185 (2001).

[58] H. Furusawa, K. Namba, H. Nakahara, C. Tanaka, Y. Yasuda, E. Hirabara, M. Imahariyama, K. Komaki, "The evolving non-surgical ablation of breast cancer: MR guided focused ultrasound (MRgFUS)," Breast Cancer **14**, 55-58 (2007).

[59] D. Gianfelice, A. Khiat, M. Amara, A. Belblidia, Y. Boulanger, "MR imaging-guided focused US ablation of breast cancer: histopathologic assessment of effectiveness-- initial experience," Radiology **227**, 849-855 (2003).

[60] R. Chopra, A. Colquhoun, M. Burtnyk, A. N'Djin W, I. Kobelevskiy, A. Boyes, K. Siddiqui, H. Foster, L. Sugar, M.A. Haider, M. Bronskill, L. Klotz, "MR Imaging-controlled Transurethral Ultrasound Therapy for Conformal Treatment of Prostate Tissue: Initial Feasibility in Humans," Radiology **265**, 303-313 (2012).

[61] K. Siddiqui, R. Chopra, S. Vedula, L. Sugar, M. Haider, A. Boyes, M. Musquera, M. Bronskill, L. Klotz, "MRI-guided transurethral ultrasound therapy of the prostate gland using real-time thermal mapping: initial studies," Urology **76**, 1506-1511 (2010).

[62] C. Li, W. Zhang, W. Fan, J. Huang, F. Zhang, P. Wu, "Noninvasive treatment of malignant bone tumors using high-intensity focused ultrasound," Cancer **116**, 3934-3942 (2010).

[63] D. Gianfelice, C. Gupta, W. Kucharczyk, P. Bret, D. Havill, M. Clemons, "Palliative treatment of painful bone metastases with MR imaging--guided focused ultrasound," Radiology **249**, 355-363 (2008).

[64] B. Liberman, D. Gianfelice, Y. Inbar, A. Beck, T. Rabin, N. Shabshin, G. Chander, S. Hengst, R. Pfeffer, A. Chechick, A. Hanannel, O. Dogadkin, R. Catane, "Pain palliation in patients with bone metastases using MR-guided focused ultrasound surgery: a multicenter study," Ann Surg Oncol **16**, 140-146 (2009).

[65] Z. Ram, Z.R. Cohen, S. Harnof, S. Tal, M. Faibel, D. Nass, S.E. Maier, M. Hadani, Y. Mardor, "Magnetic resonance imaging-guided, high-intensity focused ultrasound for brain tumor therapy," Neurosurgery **59**, 949-955; discussion 955-946 (2006).

[66] N. McDannold, G.T. Clement, P. Black, F. Jolesz, K. Hynynen, "Transcranial magnetic resonance imaging- guided focused ultrasound surgery of brain tumors: initial findings in 3 patients," Neurosurgery **66**, 323-332; discussion 332 (2010).

[67] E. Martin, D. Jeanmonod, A. Morel, E. Zadicario, B. Werner, "High-intensity focused ultrasound for noninvasive functional neurosurgery," Ann Neurol **66**, 858-861 (2009).

[68] D. Jeanmonod, B. Werner, A. Morel, L. Michels, E. Zadicario, G. Schiff, E. Martin, "Transcranial magnetic resonance imaging-guided focused ultrasound: noninvasive central lateral thalamotomy for chronic neuropathic pain," Neurosurg Focus **32**, E1 (2012).

[69] W.J. Tyler, Y. Tufail, S. Pati, "Pain: Noninvasive functional neurosurgery using ultrasound," Nat Rev Neurol **6**, 13-14 (2010).

[70] K. Hynynen, D.J. Watmough, J.R. Mallard, "Design of ultrasonic transducers for local hyperthermia," Ultrasound Med Biol **7**, 397-402 (1981).

[71] K. Hynynen, W.R. Freund, H.E. Cline, A.H. Chung, R.D. Watkins, J.P. Vetro, F.A. Jolesz, "A clinical, noninvasive, MR imaging-monitored ultrasound surgery method," Radiographics **16**, 185-195 (1996).

[72] C. Mougenot, B. Quesson, B.D. de Senneville, P.L. de Oliveira, S. Sprinkhuizen, J. Palussiere, N. Grenier, C.T. Moonen, "Three-dimensional spatial and temporal temperature control with MR thermometry-guided focused ultrasound (MRgHIFU)," Magn Reson Med **61**, 603-614 (2009).

[73] J.K. Enholm, M.O. Köhler, B. Quesson, C. Mougenot, C.T. Moonen, S.D. Sokka, "Improved volumetric MR-HIFU ablation by robust binary feedback control," IEEE Trans Biomed Eng **57**, 103-113 (2010).

[74] D.R. Daum, K. Hynynen, "A 256-element ultrasonic phased array system for the treatment of large volumes of deep seated tissue," IEEE Trans Ultrason Ferroelectr Freq Control **46**, 1254-1268 (1999).

[75] B. Hildebrandt, P. Wust, O. Ahlers, A. Dieing, G. Sreenivasa, T. Kerner, R. Felix, H. Riess, "The cellular and molecular basis of hyperthermia," Crit Rev Oncol Hematol **43**, 33-56 (2002).

[76] C.W. Song, "Effect of local hyperthermia on blood flow and microenvironment: a review," Cancer Res **44**, 4721s-4730s (1984).

[77] D.R. Daum, K. Hynynen, "Thermal dose optimization via temporal switching in ultrasound surgery," IEEE Trans Ultrason Ferroelectr Freq Control **45**, 208-215 (1998).

[78] E.S. Ebbini, C.A. Cain, "Multiple-focus ultrasound phased-array pattern synthesis: optimal driving-signal distributions for hyperthermia," IEEE Trans Ultrason Ferroelectr Freq Control **36**, 540-548 (1989).

[79] X. Fan, K. Hynynen, "Control of the necrosed tissue volume during noninvasive ultrasound surgery using a 16-element phased array," Med Phys **22**, 297-306 (1995).
[80] D. Arora, D. Cooley, T. Perry, J. Guo, A. Richardson, J. Moellmer, R. Hadley, D. Parker, M. Skliar, R.B. Roemer, "MR thermometry-based feedback control of efficacy and safety in minimum-time thermal therapies: phantom and in-vivo evaluations," Int J Hyperthermia **22**, 29-42 (2006).
[81] R. Salomir, J. Palussiere, F.C. Vimeux, J.A. de Zwart, B. Quesson, M. Gauchet, P. Lelong, J. Pergrale, N. Grenier, C.T. Moonen, "Local hyperthermia with MR-guided focused ultrasound: spiral trajectory of the focal point optimized for temperature uniformity in the target region," J Magn Reson Imaging **12**, 571-583 (2000).
[82] R. Salomir, F.C. Vimeux, J.A. de Zwart, N. Grenier, C.T. Moonen, "Hyperthermia by MR-guided focused ultrasound: accurate temperature control based on fast MRI and a physical model of local energy deposition and heat conduction," Magn Reson Med **43**, 342-347 (2000).
[83] F.C. Vimeux, J.A. De Zwart, J. Palussiere, R. Fawaz, C. Delalande, P. Canioni, N. Grenier, C.T. Moonen, "Real-time control of focused ultrasound heating based on rapid MR thermometry," Invest Radiol **34**, 190-193 (1999).
[84] P.M. Krawczyk, B. Eppink, J. Essers, J. Stap, H. Rodermond, H. Odijk, A. Zelensky, C. van Bree, L.J. Stalpers, M.R. Buist, T. Soullie, J. Rens, H.J. Verhagen, M.J. O'Connor, N.A. Franken, T.L. Ten Hagen, R. Kanaar, J.A. Aten, "Mild hyperthermia inhibits homologous recombination, induces BRCA2 degradation, and sensitizes cancer cells to poly (ADP-ribose) polymerase-1 inhibition," Proc Natl Acad Sci U S A **108**, 9851-9856 (2011).
[85] J.J. Skitzki, E.A. Repasky, S.S. Evans, "Hyperthermia as an immunotherapy strategy for cancer," Curr Opin Investig Drugs **10**, 550-558 (2009).
[86] C.J. Diederich, K. Hynynen, "Ultrasound technology for hyperthermia," Ultrasound Med Biol **25**, 871-887 (1999).
[87] P.P. Lele, "Advanced ultrasonic techniques for local tumor hyperthermia," Radiol Clin North Am **27**, 559-575 (1989).
[88] R. Strom, C. Crifo, A. Rossi-Fanelli, B. Mondovi, "Biochemical aspects of heat sensitivity of tumour cells," Recent Results Cancer Res, 7-35 (1977).
[89] R.A. Coss, W.A. Linnemans, "The effects of hyperthermia on the cytoskeleton: a review," Int J Hyperthermia **12**, 173-196 (1996).
[90] A.W. Konings, A.C. Ruifrok, "Role of membrane lipids and membrane fluidity in thermosensitivity and thermotolerance of mammalian cells," Radiat Res **102**, 86-98 (1985).
[91] R.A. Coss, W.C. Dewey, J.R. Bamburg, "Effects of hyperthermia on dividing Chinese hamster ovary cells and on microtubules in vitro," Cancer Res **42**, 1059-1071 (1982).
[92] B.V. Harmon, A.M. Corder, R.J. Collins, G.C. Gobe, J. Allen, D.J. Allan, J.F. Kerr, "Cell death induced in a murine mastocytoma by 42-47 degrees C heating in vitro: evidence that the form of death changes from apoptosis to necrosis above a critical heat load," Int J Radiat Biol **58**, 845-858 (1990).
[93] C. Streffer, "Aspects of metabolic change after hyperthermia," Recent Results Cancer Res **107**, 7-16 (1988).
[94] P.W. Burgman, H.H. Kampinga, A.W. Konings, "Possible role of localized protein denaturation in the mechanism of induction of thermotolerance by heat, sodium-arsenite and ethanol," Int J Hyperthermia **9**, 151-162 (1993).
[95] H.H. Kampinga, "Thermotolerance in mammalian cells. Protein denaturation and aggregation, and stress proteins," J Cell Sci **104 (Pt 1)**, 11-17 (1993).
[96] M. Jaattela, "Heat shock proteins as cellular lifeguards," Ann Med **31**, 261-271 (1999).
[97] J. Dahm-Daphi, I. Brammer, E. Dikomey, "Heat effects on the repair of DNA double-strand breaks in CHO cells," Int J Radiat Biol **72**, 171-179 (1997).
[98] J.M. Bull, "An update on the anticancer effects of a combination of chemotherapy and hyperthermia," Cancer Res **44**, 4853s-4856s (1984).
[99] O. Dahl, "Interaction of hyperthermia and chemotherapy," Recent Results Cancer Res **107**, 157-169 (1988).

[100] H. Maeda, L.W. Seymour, Y. Miyamoto, "Conjugates of anticancer agents and polymers: advantages of macromolecular therapeutics in vivo," Bioconjug Chem **3**, 351-362 (1992).

[101] Y. Matsumura, H. Maeda, "A new concept for macromolecular therapeutics in cancer chemotherapy: mechanism of tumoritropic accumulation of proteins and the antitumor agent smancs," Cancer Res **46**, 6387-6392 (1986).

[102] L. Li, T.L. ten Hagen, D. Schipper, T.M. Wijnberg, G.C. van Rhoon, A.M. Eggermont, L.H. Lindner, G.A. Koning, "Triggered content release from optimized stealth thermosensitive liposomes using mild hyperthermia," J Control Release **143**, 274-279 (2010).

[103] R.D. Issels, J. Mittermuller, A. Gerl, W. Simon, A. Ortmaier, C. Denzlinger, H. Sauer, W. Wilmanns, "Improvement of local control by regional hyperthermia combined with systemic chemotherapy (ifosfamide plus etoposide) in advanced sarcomas: updated report on 65 patients," J Cancer Res Clin Oncol **117 Suppl 4**, S141-147 (1991).

[104] B. Hildebrandt, P. Wust, B. Rau, P. Schlag, H. Riess, "Regional hyperthermia for rectal cancer," Lancet **356**, 771-772 (2000).

[105] J.R. Oleson, T.V. Samulski, K.A. Leopold, S.T. Clegg, M.W. Dewhirst, R.K. Dodge, S.L. George, "Sensitivity of hyperthermia trial outcomes to temperature and time: implications for thermal goals of treatment," Int J Radiat Oncol Biol Phys **25**, 289-297 (1993).

[106] P. Wust, J. Gellermann, B. Rau, J. Loffel, A. Speidel, H. Stahl, H. Riess, T.J. Vogl, R. Felix, P.M. Schlag, "Hyperthermia in the multimodal therapy of advanced rectal carcinomas," Recent Results Cancer Res **142**, 281-309 (1996).

[107] P. Wust, H. Stahl, K. Dieckmann, S. Scheller, J. Loffel, H. Riess, J. Bier, V. Jahnke, R. Felix, "Local hyperthermia of N2/N3 cervical lymph node metastases: correlationof technical/thermal parameters and response," Int J Radiat Oncol Biol Phys **34**, 635-646 (1996).

[108] B. Rau, P. Wust, W. Tilly, J. Gellermann, C. Harder, H. Riess, V. Budach, R. Felix, P.M. Schlag, "Preoperative radiochemotherapy in locally advanced or recurrent rectal cancer: regional radiofrequency hyperthermia correlates with clinical parameters," Int J Radiat Oncol Biol Phys **48**, 381-391 (2000).

[109] T.S. Lawrence, R.K. Ten Haken, A. Giaccia, "Principles of Radiation Oncology," in *Cancer: Principles and Practice of Oncology,* edited by V.T. DeVita, T.S. Lawrence, S.A. Rosenberg (Lippincott Williams & Wilkins, Philadelphia, 2008).

[110] R.R. Patel, D.W. Arthur, "The emergence of advanced brachytherapy techniques for common malignancies," Hematol Oncol Clin North Am **20**, 97-118 (2006).

[111] M.D. Mills, R.E. Meyn, "Hyperthermic potentiation of unrejoined DNA strand breaks following irradiation," Radiat Res **95**, 327-338 (1983).

[112] S.H. Kim, J.H. Kim, E.W. Hahn, "The enhanced killing of irradiated HeLa cells in synchronous culture by hyperthermia," Radiat Res **66**, 337-345 (1976).

[113] W.A. Denny, "Prodrug strategies in cancer therapy," Eur J Med Chem **36**, 577-595 (2001).

[114] C.W. Song, H. Park, R.J. Griffin, "Improvement of tumor oxygenation by mild hyperthermia," Radiat Res **155**, 515-528 (2001).

[115] X. Sun, L. Xing, C.C. Ling, G.C. Li, "The effect of mild temperature hyperthermia on tumour hypoxia and blood perfusion: relevance for radiotherapy, vascular targeting and imaging," Int J Hyperthermia **26**, 224-231 (2010).

[116] J. Overgaard, D. Gonzalez Gonzalez, M.C. Hulshof, G. Arcangeli, O. Dahl, O. Mella, S.M. Bentzen, "Hyperthermia as an adjuvant to radiation therapy of recurrent or metastatic malignant melanoma. A multicentre randomized trial by the European Society for Hyperthermic Oncology," Int J Hyperthermia **12**, 3-20 (1996).

[117] C.A. Perez, T. Pajak, B. Emami, N.B. Hornback, L. Tupchong, P. Rubin, "Randomized phase III study comparing irradiation and hyperthermia with irradiation alone in superficial measurable tumors. Final report by the Radiation Therapy Oncology Group," Am J Clin Oncol **14**, 133-141 (1991).

[118] B. Emami, C. Scott, C.A. Perez, S. Asbell, P. Swift, P. Grigsby, A. Montesano, P. Rubin, W. Curran, J. Delrowe, H. Arastu, K. Fu, E. Moros, "Phase III study of interstitial thermoradiotherapy compared with interstitial radiotherapy alone in the treatment of recurrent or persistent human tumors. A prospectively controlled randomized study by the Radiation Therapy Group," Int J Radiat Oncol Biol Phys **34**, 1097-1104 (1996).

[119] P.K. Sneed, P.R. Stauffer, M.W. McDermott, C.J. Diederich, K.R. Lamborn, M.D. Prados, S. Chang, K.A. Weaver, L. Spry, M.K. Malec, S.A. Lamb, B. Voss, R.L. Davis, W.M. Wara, D.A. Larson, T.L. Phillips, P.H. Gutin, "Survival benefit of hyperthermia in a prospective randomized trial of brachytherapy boost +/- hyperthermia for glioblastoma multiforme," Int J Radiat Oncol Biol Phys **40**, 287-295 (1998).

[120] K. Kitamura, H. Kuwano, M. Watanabe, T. Nozoe, M. Yasuda, K. Sumiyoshi, M. Saku, K. Sugimachi, "Prospective randomized study of hyperthermia combined with chemoradiotherapy for esophageal carcinoma," J Surg Oncol **60**, 55-58 (1995).

[121] Y. Harima, K. Nagata, K. Harima, V.V. Ostapenko, Y. Tanaka, S. Sawada, "A randomized clinical trial of radiation therapy versus thermoradiotherapy in stage IIIB cervical carcinoma," Int J Hyperthermia **17**, 97-105 (2001).

[122] J. van der Zee, D. Gonzalez Gonzalez, G.C. van Rhoon, J.D. van Dijk, W.L. van Putten, A.A. Hart, "Comparison of radiotherapy alone with radiotherapy plus hyperthermia in locally advanced pelvic tumours: a prospective, randomised, multicentre trial. Dutch Deep Hyperthermia Group," Lancet **355**, 1119-1125 (2000).

[123] M.W. Dewhirst, "Thermal dosimetry," in *Thermoradiotherapy and thermochemotherapy*, *Vol. 1,* edited by M. Seegenschmiedt, P. Fessenden, C.C. Vernon (Springer Verlag, Berlin, 1995), pp. 123-138.

[124] M.H. Seegenschmiedt, P. Martus, R. Fietkau, H. Iro, L.W. Brady, R. Sauer, "Multivariate analysis of prognostic parameters using interstitial thermoradiotherapy (IHT-IRT): tumor and treatment variables predict outcome," Int J Radiat Oncol Biol Phys **29**, 1049-1063 (1994).

[125] J. Crawford, D.C. Dale, G.H. Lyman, "Chemotherapy-induced neutropenia: risks, consequences, and new directions for its management," Cancer **100**, 228-237 (2004).

[126] R.M. Trueb, "Chemotherapy-induced alopecia," Curr Opin Support Palliat Care **4**, 281-284 (2010).

[127] T.S. Herman, B.A. Teicher, A. Varshney, V. Khandekar, T. Brann, "Effect of hypoxia and acidosis on the cytotoxicity of mitoxantrone, bisantrene and amsacrine and their platinum complexes at normal and hyperthermic temperatures," Anticancer Res **12**, 827-836 (1992).

[128] S.A. Holden, B.A. Teicher, T.S. Herman, "Effect of environmental conditions (pH, oxygenation, and temperature) on misonidazole cytotoxicity and radiosensitization in vitro and in vivo in FSaIIC fibrosarcoma," Int J Radiat Oncol Biol Phys **20**, 1031-1038 (1991).

[129] B.A. Teicher, T.S. Herman, S.A. Holden, M.B. Rudolph, "Effect of oxygenation, pH and hyperthermia on RSU-1069 in vitro and in vivo with radiation in the FSaIIC murine fibrosarcoma," Cancer Lett **59**, 109-117 (1991).

[130] R.K. Jain, "Normalization of tumor vasculature: an emerging concept in antiangiogenic therapy," Science **307**, 58-62 (2005).

[131] O. Tredan, C.M. Galmarini, K. Patel, I.F. Tannock, "Drug resistance and the solid tumor microenvironment," J Natl Cancer Inst **99**, 1441-1454 (2007).

[132] R. Hamazoe, M. Maeta, N. Kaibara, "Intraperitoneal thermochemotherapy for prevention of peritoneal recurrence of gastric cancer. Final results of a randomized controlled study," Cancer **73**, 2048-2052 (1994).

[133] L. Hafstrom, C.M. Rudenstam, E. Blomquist, C. Ingvar, P.E. Jonsson, B. Lagerlof, C. Lindholm, U. Ringborg, G. Westman, L. Ostrup, "Regional hyperthermic perfusion with melphalan after surgery for recurrent malignant melanoma of the extremities. Swedish Melanoma Study Group," J Clin Oncol **9**, 2091-2094 (1991).

134 H.S. Koops, M. Vaglini, S. Suciu, B.B. Kroon, J.F. Thompson, J. Gohl, A.M. Eggermont, F. Di Filippo, E.T. Krementz, D. Ruiter, F.J. Lejeune, "Prophylactic isolated limb perfusion for localized, high-risk limb melanoma: results of a multicenter randomized phase III trial. European Organization for Research and Treatment of Cancer Malignant Melanoma Cooperative Group Protocol 18832, the World Health Organization Melanoma Program Trial 15, and the North American Perfusion Group Southwest Oncology Group-8593," J Clin Oncol **16**, 2906-2912 (1998).

135 D.C. Drummond, O. Meyer, K. Hong, D.B. Kirpotin, D. Papahadjopoulos, "Optimizing liposomes for delivery of chemotherapeutic agents to solid tumors," Pharmacol Rev **51**, 691-743 (1999).

136 R.K. Jain, T. Stylianopoulos, "Delivering nanomedicine to solid tumors," Nat Rev Clin Oncol **7**, 653-664 (2010).

137 R.M. Staruch, M. Ganguly, I.F. Tannock, K. Hynynen, R. Chopra, "Enhanced drug delivery in rabbit VX2 tumours using thermosensitive liposomes and MRI-controlled focused ultrasound hyperthermia," Int J Hyperthermia **28**, 776-787 (2012).

138 F. Yuan, M. Leunig, S.K. Huang, D.A. Berk, D. Papahadjopoulos, R.K. Jain, "Microvascular permeability and interstitial penetration of sterically stabilized (stealth) liposomes in a human tumor xenograft," Cancer Res **54**, 3352-3356 (1994).

139 A.A. Manzoor, L.H. Lindner, C.D. Landon, J.Y. Park, A.J. Simnick, M.R. Dreher, S. Das, G. Hanna, W. Park, A. Chilkoti, G.A. Koning, T.L. Ten Hagen, D. Needham, M.W. Dewhirst, "Overcoming Limitations in Nanoparticle Drug Delivery: Triggered, Intravascular Release to Improve Drug Penetration into Tumors," Cancer Res **72**, 5566-5575 (2012).

140 D.W. Northfelt, F.J. Martin, P. Working, P.A. Volberding, J. Russell, M. Newman, M.A. Amantea, L.D. Kaplan, "Doxorubicin encapsulated in liposomes containing surface-bound polyethylene glycol: pharmacokinetics, tumor localization, and safety in patients with AIDS-related Kaposi's sarcoma," J Clin Pharmacol **36**, 55-63 (1996).

141 A.H. Negussie, J.L. Miller, G. Reddy, S.K. Drake, B.J. Wood, M.R. Dreher, "Synthesis and in vitro evaluation of cyclic NGR peptide targeted thermally sensitive liposome," J Control Release **143**, 265-273 (2010).

142 K.E. Lokling, S.L. Fossheim, J. Klaveness, R. Skurtveit, "Biodistribution of pH-responsive liposomes for MRI and a novel approach to improve the pH-responsiveness," J Control Release **98**, 87-95 (2004).

143 T. Spratt, B. Bondurant, D.F. O'Brien, "Rapid release of liposomal contents upon photoinitiated destabilization with UV exposure," Biochim Biophys Acta **1611**, 35-43 (2003).

144 S.S. Jensen, T.L. Andresen, J. Davidsen, P. Hoyrup, S.D. Shnyder, M.C. Bibby, J.H. Gill, K. Jorgensen, "Secretory phospholipase A2 as a tumor-specific trigger for targeted delivery of a novel class of liposomal prodrug anticancer etherlipids," Mol Cancer Ther **3**, 1451-1458 (2004).

145 L.H. Lindner, M.E. Eichhorn, H. Eibl, N. Teichert, M. Schmitt-Sody, R.D. Issels, M. Dellian, "Novel temperature-sensitive liposomes with prolonged circulation time," Clinical cancer research : an official journal of the American Association for Cancer Research **10**, 2168-2178 (2004).

146 Celsion, "A Study of ThermoDox™ in Combination With Radiofrequency Ablation (RFA) in Primary and Metastatic Tumors of the Liver," *Vol. 2012* (In: ClinicalTrials.gov [Internet]), pp. NLM Identifier: NCT00441376.

147 Celsion, "Phase 3 Study of ThermoDox With Radiofrequency Ablation (RFA) in Treatment of Hepatocellular Carcinoma (HCC)," *Vol. 2012* (In: ClinicalTrials.gov [Internet]), pp. NLM Identifier: NCT00617981.

148 Celsion, "MRI Guided High Intensity Focused Ultrasound (HIFU) and ThermoDox for Palliation of Painful Bone Metastases," *Vol. 2012* (In: ClinicalTrials.gov [Internet]), pp. NLM Identifier: NCT01640847.

149 Celsion, "Phase 2 Study of Thermodox as Adjuvant Therapy With Radiofrequency Ablation (RFA) in Treatment of Colorectal Liver Metastases (CRLM) (ABLATE)," *Vol. 2012* (In: ClinicalTrials.gov [Internet]), pp. NLM Identifier: NCT01464593.

[150] M. Hossann, M. Wiggenhorn, A. Schwerdt, K. Wachholz, N. Teichert, H. Eibl, R.D. Issels, L.H. Lindner, "In vitro stability and content release properties of phosphatidylglyceroglycerol containing thermosensitive liposomes," Biochim Biophys Acta **1768**, 2491-2499 (2007).

[151] S.S. Abdullah, J.B. Pialat, M. Wiart, F. Duboeuf, J.Y. Mabrut, B. Bancel, A. Rode, C. Ducerf, J. Baulieux, Y. Berthezene, "Characterization of hepatocellular carcinoma and colorectal liver metastasis by means of perfusion MRI," J Magn Reson Imaging **28**, 390-395 (2008).

[152] L. Ludemann, D. Prochnow, T. Rohlfing, T. Franiel, C. Warmuth, M. Taupitz, H. Rehbein, D. Beyersdorff, "Simultaneous quantification of perfusion and permeability in the prostate using dynamic contrast-enhanced magnetic resonance imaging with an inversion-prepared dual-contrast sequence," Ann Biomed Eng **37**, 749-762 (2009).

[153] C. Freccero, F. Holmlund, S. Bornmyr, J. Castenfors, A.M. Johansson, G. Sundkvist, H. Svensson, P. Wollmer, "Laser Doppler perfusion monitoring of skin blood flow at different depths in finger and arm upon local heating," Microvasc Res **66**, 183-189 (2003).

[154] C. Tilcock, E. Unger, P. Cullis, P. MacDougall, "Liposomal Gd-DTPA: preparation and characterization of relaxivity," Radiology **171**, 77-80 (1989).

[155] S.H. Koenig, Q.F. Ahkong, R.D. Brown, 3rd, M. Lafleur, M. Spiller, E. Unger, C. Tilcock, "Permeability of liposomal membranes to water: results from the magnetic field dependence of T1 of solvent protons in suspensions of vesicles with entrapped paramagnetic ions," Magn Reson Med **23**, 275-286 (1992).

[156] W.L. Nyborg, R.B. Steele, "Temperature elevation in a beam of ultrasound," Ultrasound Med Biol **9**, 611-620 (1983).

[157] M.D.P.D. Peter M. Doubilet, P.M.D.C.B. Benson, *Atlas of Ultrasound in Obstetrics and Gynecology*, 5th ed. (Lippincott Williams & Wilkins, Philadelphia, 2003).

[158] W. Wood, A.L. Loomis, "The physical and biological effects of high-frequency sound waves of great intensity," Phil Mag S, 417-436 (1927).

[159] T.R. Nelson, J.B. Fowlkes, J.S. Abramowicz, C.C. Church, "Ultrasound biosafety considerations for the practicing sonographer and sonologist," Journal of ultrasound in medicine : official journal of the American Institute of Ultrasound in Medicine **28**, 139-150 (2009).

[160] G. ter Haar, "Ultrasound focal beam surgery," Ultrasound Med Biol **21**, 1089-1100 (1995).

[161] F. Wu, W.Z. Chen, J. Bai, J.Z. Zou, Z.L. Wang, H. Zhu, Z.B. Wang, "Pathological changes in human malignant carcinoma treated with high-intensity focused ultrasound," Ultrasound Med Biol **27**, 1099-1106 (2001).

[162] G. ter Haar, C. Coussios, "High intensity focused ultrasound: physical principles and devices," Int J Hyperthermia **23**, 89-104 (2007).

[163] G.R. Schade, T.L. Hall, W.W. Roberts, "Urethral-sparing histotripsy of the prostate in a canine model," Urology **80**, 730-735 (2012).

[164] M. Demirbas, M. Samli, M. Karalar, A.C. Kose, "Extracorporeal shockwave lithotripsy for ureteral stones: twelve years of experience with 2836 patients at a single center," Urol J **9**, 557-561 (2012).

[165] A.V. Alexandrov, C.A. Molina, J.C. Grotta, Z. Garami, S.R. Ford, J. Alvarez-Sabin, J. Montaner, M. Saqqur, A.M. Demchuk, L.A. Moyé, M.D. Hill, A.W. Wojner, "Ultrasound-Enhanced Systemic Thrombolysis for Acute Ischemic Stroke," New England Journal of Medicine **351**, 2170-2178 (2004).

[166] F.A. Jolesz, K.H. Hynynen, *MRI-Guided Focused Ultrasound Surgery*. (Taylor & Francis, 2007).

[167] D. Cathignol, O.A. Sapozhnikov, Y. Theillere, "Comparison of acoustic fields radiated from piezoceramic and piezocomposite focused radiators," J Acoust Soc Am **105**, 2612-2617 (1999).

[168] E.S. Ebbini, C.A. Cain, "A spherical-section ultrasound phased array applicator for deep localized hyperthermia," IEEE Trans Biomed Eng **38**, 634-643 (1991).

[169] M. Pernot, J.F. Aubry, M. Tanter, J.L. Thomas, M. Fink, "High power transcranial beam steering for ultrasonic brain therapy," Phys Med Biol **48**, 2577-2589 (2003).

[170] H.E. Cline, K. Hynynen, R.D. Watkins, W.J. Adams, J.F. Schenck, R.H. Ettinger, W.R. Freund, J.P. Vetro, F.A. Jolesz, "Focused US system for MR imaging-guided tumor ablation," Radiology **194**, 731-737 (1995).

171 I.H. Rivens, R.L. Clarke, G.R. ter Haar, "Design of focused ultrasound surgery transducers," IEEE Transactions on Ultrasonics Ferroelectrics and Frequency Control **43**, 1023-1031 (1996).

172 *Therapeutic Ultrasound : Mechanisms to Applications*, 1st ed. (Nova Science Publishers, New York, 2010).

173 S.A. Goss, R.L. Johnston, F. Dunn, "Comprehensive compilation of empirical ultrasonic properties of mammalian tissues," J Acoust Soc Am **64**, 423-457 (1978).

174 G.D. Ludwig, "The Velocity of Sound through Tissues and the Acoustic Impedance of Tissues," J Acoust Soc Am **22**, 862-866 (1950).

175 F.A. Duck, *Physical properties of tissue: a comprehensive reference book*. (Academic Press, 1990).

176 F.M. Fennessy, C.M. Tempany, N.J. McDannold, M.J. So, G. Hesley, B. Gostout, H.S. Kim, G.A. Holland, D.A. Sarti, K. Hynynen, F.A. Jolesz, E.A. Stewart, "Uterine leiomyomas: MR imaging-guided focused ultrasound surgery--results of different treatment protocols," Radiology **243**, 885-893 (2007).

177 C.R. Hill, "Optimum acoustic frequency for focused ultrasound surgery," Ultrasound Med Biol **20**, 271-277 (1994).

178 I.P. Wharton, I.H. Rivens, G.R. Ter Haar, D.J. Gilderdale, D.J. Collins, J.W. Hand, P.D. Abel, N.M. deSouza, "Design and development of a prototype endocavitary probe for high-intensity focused ultrasound delivery with integrated magnetic resonance imaging," J Magn Reson Imaging **25**, 548-556 (2007).

179 L.R. Gavrilov, J.W. Hand, "A theoretical assessment of the relative performance of spherical phased arrays for ultrasound surgery," IEEE Trans Ultrason Ferroelectr Freq Control **47**, 125-139 (2000).

180 S. Umemura, C.A. Cain, "The sector-vortex phased array: acoustic field synthesis for hyperthermia," IEEE Trans Ultrason Ferroelectr Freq Control **36**, 249-257 (1989).

181 J.Y. Chapelon, D. Cathignol, C. Cain, E. Ebbini, J.U. Kluiwstra, O.A. Sapozhnikov, G. Fleury, R. Berriet, L. Chupin, J.L. Guey, "New piezoelectric transducers for therapeutic ultrasound," Ultrasound Med Biol **26**, 153-159 (2000).

182 E.S. Ebbini, S.I. Umemura, M. Ibbini, C.A. Cain, "A cylindrical-section ultrasound phased-array applicator for hyperthermia cancer therapy," IEEE Trans Ultrason Ferroelectr Freq Control **35**, 561-572 (1988).

183 S. Umemura, C.A. Cain, "Acoustical evaluation of a prototype sector-vortex phased-array applicator," IEEE Trans Ultrason Ferroelectr Freq Control **39**, 32-38 (1992).

184 F. Dupenloup, J.Y. Chapelon, D. Cathignol, O.A. Sapozhnikov, "Reduction of the grating lobes of annular arrays used in focused ultrasound surgery," IEEE Trans Ultrason Ferroelectr Freq Control **43**, 991-998 (1996).

185 H.L. Liu, N. McDannold, K. Hynynen, "Focal beam distortion and treatment planning in abdominal focused ultrasound surgery," Med Phys **32**, 1270-1280 (2005).

186 W.D. O'Brien, Jr., "Ultrasound-biophysics mechanisms," Prog Biophys Mol Biol **93**, 212-255 (2007).

187 K. Hynynen, "The threshold for thermally significant cavitation in dog's thigh muscle in vivo," Ultrasound Med Biol **17**, 157-169 (1991).

188 S.D. Sokka, R. King, K. Hynynen, "MRI-guided gas bubble enhanced ultrasound heating in in vivo rabbit thigh," Phys Med Biol **48**, 223-241 (2003).

189 G. ter Haar, "Basic physics of therapeutic ultrasound," Physiotherapy **64**, 100-103 (1978).

190 C.K. Holland, R.E. Apfel, "Thresholds for transient cavitation produced by pulsed ultrasound in a controlled nuclei environment," J Acoust Soc Am **88**, 2059-2069 (1990).

191 M.S. Canney, M.R. Bailey, L.A. Crum, V.A. Khokhlova, O.A. Sapozhnikov, "Acoustic characterization of high intensity focused ultrasound fields: a combined measurement and modeling approach," J Acoust Soc Am **124**, 2406-2420 (2008).

192 D. Dalecki, E.L. Carstensen, K.J. Parker, D.R. Bacon, "Absorption of finite amplitude focused ultrasound," J Acoust Soc Am **89**, 2435-2447 (1991).

[193] K. Hynynen, "Demonstration of enhanced temperature elevation due to nonlinear propagation of focussed ultrasound in dog's thigh in vivo," Ultrasound in Medicine & Biology **13**, 85-91 (1987).

[194] E. Filonenko, V. Khokhlova, "Effect of acoustic nonlinearity on heating of biological tissue by high-intensity focused ultrasound," Acoustical Physics **47**, 468-475 (2001).

[195] M.S. Canney, V.A. Khokhlova, O.V. Bessonova, M.R. Bailey, L.A. Crum, "Shock-induced heating and millisecond boiling in gels and tissue due to high intensity focused ultrasound," Ultrasound Med Biol **36**, 250-267 (2010).

[196] H.H. Pennes, "Analysis of tissue and arterial blood temperatures in the resting human forearm," J Appl Physiol **1**, 93-122 (1948).

[197] J.W. Valvano, "Tissue Thermal Properties And Perfusion," in *Optical-Thermal Response of Laser-Irradiated Tissue,* edited by A.J. Welch, M.J.C. Van Gemert (Springer, Dordrecht, 2011).

[198] M.J. Choi, S.R. Guntur, J.M. Lee, D.G. Paeng, K.I. Lee, A. Coleman, "Changes in ultrasonic properties of liver tissue in vitro during heating-cooling cycle concomitant with thermal coagulation," Ultrasound Med Biol **37**, 2000-2012 (2011).

[199] I. Dragonu, P.L. de Oliveira, C. Laurent, C. Mougenot, N. Grenier, C.T. Moonen, B. Quesson, "Non-invasive determination of tissue thermal parameters from high intensity focused ultrasound treatment monitored by volumetric MRI thermometry," NMR in biomedicine **22**, 843-851 (2009).

[200] J. Lang, B. Erdmann, M. Seebass, "Impact of nonlinear heat transfer on temperature control in regional hyperthermia," IEEE Trans Biomed Eng **46**, 1129-1138 (1999).

[201] L. Chen, G. ter Haar, C.R. Hill, M. Dworkin, P. Carnochan, H. Young, J.P. Bensted, "Effect of blood perfusion on the ablation of liver parenchyma with high-intensity focused ultrasound," Phys Med Biol **38**, 1661-1673 (1993).

[202] Z. Liu, M. Ahmed, A. Sabir, S. Humphries, S.N. Goldberg, "Computer modeling of the effect of perfusion on heating patterns in radiofrequency tumor ablation," Int J Hyperthermia **23**, 49-58 (2007).

[203] S.A. Sapareto, W.C. Dewey, "Thermal dose determination in cancer therapy," Int J Radiat Oncol Biol Phys **10**, 787-800 (1984).

[204] P.S. Yarmolenko, E.J. Moon, C. Landon, A. Manzoor, D.W. Hochman, B.L. Viglianti, M.W. Dewhirst, "Thresholds for thermal damage to normal tissues: an update," Int J Hyperthermia **27**, 320-343 (2011).

[205] N.J. McDannold, R.L. King, F.A. Jolesz, K.H. Hynynen, "Usefulness of MR imaging-derived thermometry and dosimetry in determining the threshold for tissue damage induced by thermal surgery in rabbits," Radiology **216**, 517-523 (2000).

[206] A.H. Chung, F.A. Jolesz, K. Hynynen, "Thermal dosimetry of a focused ultrasound beam in vivo by magnetic resonance imaging," Med Phys **26**, 2017-2026 (1999).

[207] J.D. Hazle, R.J. Stafford, R.E. Price, "Magnetic resonance imaging-guided focused ultrasound thermal therapy in experimental animal models: correlation of ablation volumes with pathology in rabbit muscle and VX2 tumors," J Magn Reson Imaging **15**, 185-194 (2002).

[208] E.L. Jones, J.R. Oleson, L.R. Prosnitz, T.V. Samulski, Z. Vujaskovic, D. Yu, L.L. Sanders, M.W. Dewhirst, "Randomized trial of hyperthermia and radiation for superficial tumors," J Clin Oncol **23**, 3079-3085 (2005).

[209] D.E. Thrall, S.M. LaRue, D. Yu, T. Samulski, L. Sanders, B. Case, G. Rosner, C. Azuma, J. Poulson, A.F. Pruitt, W. Stanley, M.L. Hauck, L. Williams, P. Hess, M.W. Dewhirst, "Thermal dose is related to duration of local control in canine sarcomas treated with thermoradiotherapy," Clinical cancer research : an official journal of the American Association for Cancer Research **11**, 5206-5214 (2005).

[210] A. Meshorer, S.D. Prionas, L.F. Fajardo, J.L. Meyer, G.M. Hahn, A.A. Martinez, "The effects of hyperthermia on normal mesenchymal tissues. Application of a histologic grading system," Arch Pathol Lab Med **107**, 328-334 (1983).

[211] McDannold, K. Hynynen, D. Wolf, G. Wolf, F. Jolesz, "MRI evaluation of thermal ablation of tumors with focused ultrasound," J Magn Reson Imaging **8**, 91-100 (1998).

[212] J.P. Yung, A. Shetty, A. Elliott, J.S. Weinberg, R.J. McNichols, A. Gowda, J.D. Hazle, R.J. Stafford, "Quantitative comparison of thermal dose models in normal canine brain," Med Phys **37**, 5313-5321 (2010).

[213] A.L. Malcolm, G.R. ter Haar, "Ablation of tissue volumes using high intensity focused ultrasound," Ultrasound Med Biol **22**, 659-669 (1996).

[214] C.R. Hill, I. Rivens, M.G. Vaughan, G.R. ter Haar, "Lesion development in focused ultrasound surgery: a general model," Ultrasound Med Biol **20**, 259-269 (1994).

[215] A. Arefiev, F. Prat, J.Y. Chapelon, J. Tavakkoli, D. Cathignol, "Ultrasound-induced tissue ablation: studies on isolated, perfused porcine liver," Ultrasound Med Biol **24**, 1033-1043 (1998).

[216] P.P. Lele, K.J. Parker, "Temperature distributions in tissues during local hyperthermia by stationary or steered beams of unfocused or focused ultrasound," Br J Cancer Suppl **5**, 108-121 (1982).

[217] J.W. Hand, C.C. Vernon, M.V. Prior, "Early experience of a commercial scanned focused ultrasound hyperthermia system," Int J Hyperthermia **8**, 587-607 (1992).

[218] E.G. Moros, R.B. Roemer, K. Hynynen, "Simulations of scanned focused ultrasound hyperthermia. the effects of scanning speed and pattern on the temperature fluctuations at the focal depth," IEEE Trans Ultrason Ferroelectr Freq Control **35**, 552-560 (1988).

[219] R.D. Peters, R.S. Hinks, R.M. Henkelman, "Ex vivo tissue-type independence in proton-resonance frequency shift MR thermometry," Magn Reson Med **40**, 454-459 (1998).

[220] X. Fan, K. Hynynen, "Ultrasound surgery using multiple sonications--treatment time considerations," Ultrasound Med Biol **22**, 471-482 (1996).

[221] D.R. Daum, N.B. Smith, R. King, K. Hynynen, "In vivo demonstration of noninvasive thermal surgery of the liver and kidney using an ultrasonic phased array," Ultrasound Med Biol **25**, 1087-1098 (1999).

[222] E.S. Ebbini, C.A. Cain, "Optimization of the intensity gain of multiple-focus phased-array heating patterns," Int J Hyperthermia **7**, 953-973 (1991).

[223] E. Guilhon, B. Quesson, F. Moraud-Gaudry, H. de Verneuil, P. Canioni, R. Salomir, P. Voisin, C.T. Moonen, "Image-guided control of transgene expression based on local hyperthermia," Mol Imaging **2**, 11-17 (2003).

[224] E. Guilhon, P. Voisin, J.A. de Zwart, B. Quesson, R. Salomir, C. Maurange, V. Bouchaud, P. Smirnov, H. de Verneuil, A. Vekris, P. Canioni, C.T. Moonen, "Spatial and temporal control of transgene expression in vivo using a heat-sensitive promoter and MRI-guided focused ultrasound," J Gene Med **5**, 333-342 (2003).

[225] S. Hey, M. Ries, C.T. Moonen, "Online temperature control of focused ultrasound heating using an adaptive PID feedback loop," Proc. Intl. Soc. Mag. Reson. Med. **19**, 1735 (2011).

[226] C. Mougenot, R. Salomir, J. Palussiere, N. Grenier, C.T. Moonen, "Automatic spatial and temporal temperature control for MR-guided focused ultrasound using fast 3D MR thermometry and multispiral trajectory of the focal point," Magn Reson Med **52**, 1005-1015 (2004).

[227] D. Arora, M.A. Minor, M. Skliar, R.B. Roemer, "Control of thermal therapies with moving power deposition field," Phys Med Biol **51**, 1201-1219 (2006).

[228] A. Vanne, K. Hynynen, "MRI feedback temperature control for focused ultrasound surgery," Phys Med Biol **48**, 31-43 (2003).

[229] D.D. Stark, W.G. Bradley, *Magnetic Resonance Imaging*. (C.V. Mosby Co., St. Louis, 1988).

[230] I.I. Rabi, J.R. Zacharias, S. Millman, P. Kusch, "A New Method of Measuring Nuclear Magnetic Moment," Physical Review **53**, 318-318 (1938).

[231] F. Bloch, W.W. Hansen, M. Packard, "Nuclear Induction," Physical Review **69**, 127-127 (1946).

[232] E.M. Purcell, H.C. Torrey, R.V. Pound, "Resonance Absorption by Nuclear Magnetic Moments in a Solid," Physical Review **69**, 37-38 (1946).

[233] C.Y. Lai, D.E. Kruse, C.F. Caskey, D.N. Stephens, P.L. Sutcliffe, K.W. Ferrara, "Noninvasive thermometry assisted by a dual-function ultrasound transducer for mild hyperthermia," IEEE Trans Ultrason Ferroelectr Freq Control **57**, 2671-2684 (2010).

[234] V. Zderic, J. Foley, W. Luo, S. Vaezy, "Prevention of post-focal thermal damage by formation of bubbles at the focus during high intensity focused ultrasound therapy," Med Phys **35**, 4292-4299 (2008).

[235] R.M. Arthur, W.L. Straube, J.W. Trobaugh, E.G. Moros, "Non-invasive estimation of hyperthermia temperatures with ultrasound," Int J Hyperthermia **21**, 589-600 (2005).
[236] M.D. Abolhassani, A. Norouzy, A. Takavar, H. Ghanaati, "Noninvasive temperature estimation using sonographic digital images," Journal of ultrasound in medicine : official journal of the American Institute of Ultrasound in Medicine **26**, 215-222 (2007).
[237] I. Rivens, A. Shaw, J. Civale, H. Morris, "Treatment monitoring and thermometry for therapeutic focused ultrasound," Int J Hyperthermia **23**, 121-139 (2007).
[238] J. De Poorter, "Noninvasive MRI thermometry with the proton resonance frequency method: study of susceptibility effects," Magn Reson Med **34**, 359-367 (1995).
[239] J.A. de Zwart, F.C. Vimeux, C. Delalande, P. Canioni, C.T. Moonen, "Fast lipid-suppressed MR temperature mapping with echo-shifted gradient-echo imaging and spectral-spatial excitation," Magn Reson Med **42**, 53-59 (1999).
[240] J.C. Hindman, "Proton Resonance Shift of Water in the Gas and Liquid States," The Journal of Chemical Physics **44**, 4582-4592 (1966).
[241] W.G. Schneider, H.J. Bernstein, J.A. Pople, "Proton Magnetic Resonance Chemical Shift of Free (Gaseous) and Associated (Liquid) Hydride Molecules," The Journal of Chemical Physics **28**, 601-607 (1958).
[242] V. Rieke, K. Butts Pauly, "MR thermometry," J Magn Reson Imaging **27**, 376-390 (2008).
[243] N. McDannold, "Quantitative MRI-based temperature mapping based on the proton resonant frequency shift: review of validation studies," Int J Hyperthermia **21**, 533-546 (2005).
[244] E.M. Delfaut, J. Beltran, G. Johnson, J. Rousseau, X. Marchandise, A. Cotten, "Fat suppression in MR imaging: techniques and pitfalls," Radiographics **19**, 373-382 (1999).
[245] C.H. Meyer, J.M. Pauly, A. Macovski, D.G. Nishimura, "Simultaneous spatial and spectral selective excitation," Magn Reson Med **15**, 287-304 (1990).
[246] F. Schick, J. Forster, J. Machann, P. Huppert, C.D. Claussen, "Highly selective water and fat imaging applying multislice sequences without sensitivity to B1 field inhomogeneities," Magn Reson Med **38**, 269-274 (1997).
[247] P.F. Van de Moortele, J. Pfeuffer, G.H. Glover, K. Ugurbil, X. Hu, "Respiration-induced B0 fluctuations and their spatial distribution in the human brain at 7 Tesla," Magn Reson Med **47**, 888-895 (2002).
[248] P. van Gelderen, J.A. de Zwart, P. Starewicz, R.S. Hinks, J.H. Duyn, "Real-time shimming to compensate for respiration-induced B0 fluctuations," Magn Reson Med **57**, 362-368 (2007).
[249] H. Rempp, P. Martirosian, A. Boss, S. Clasen, A. Kickhefel, M. Kraiger, C. Schraml, C. Claussen, P. Pereira, F. Schick, "MR temperature monitoring applying the proton resonance frequency method in liver and kidney at 0.2 and 1.5 T: segment-specific attainable precision and breathing influence," MAGMA **21**, 333-343 (2008).
[250] C.R. Wyatt, B.J. Soher, J.R. MacFall, "Correction of breathing-induced errors in magnetic resonance thermometry of hyperthermia using multiecho field fitting techniques," Med Phys **37**, 6300-6309 (2010).
[251] S. Hey, G. Maclair, B.D. de Senneville, M. Lepetit-Coiffe, Y. Berber, M.O. Köhler, B. Quesson, C.T. Moonen, M. Ries, "Online correction of respiratory-induced field disturbances for continuous MR-thermometry in the breast," Magn Reson Med **61**, 1494-1499 (2009).
[252] X. Hu, T.H. Le, T. Parrish, P. Erhard, "Retrospective estimation and correction of physiological fluctuation in functional MRI," Magn Reson Med **34**, 201-212 (1995).
[253] B. Wowk, M.C. McIntyre, J.K. Saunders, "k-Space detection and correction of physiological artifacts in fMRI," Magn Reson Med **38**, 1029-1034 (1997).
[254] J.A. de Zwart, F.C. Vimeux, J. Palussiere, R. Salomir, B. Quesson, C. Delalande, C.T. Moonen, "On-line correction and visualization of motion during MRI-controlled hyperthermia," Magn Reson Med **45**, 128-137 (2001).
[255] K.K. Vigen, B.L. Daniel, J.M. Pauly, K. Butts, "Triggered, navigated, multi-baseline method for proton resonance frequency temperature mapping with respiratory motion," Magn Reson Med **50**, 1003-1010 (2003).

[256] M.O. Köhler, B. Denis de Senneville, B. Quesson, C.T. Moonen, M. Ries, "Spectrally selective pencil-beam navigator for motion compensation of MR-guided high-intensity focused ultrasound therapy of abdominal organs," Magn Reson Med. **66**, 102-111. doi: 110.1002/mrm.22784. Epub 22011 Feb 22788. (2011).

[257] B.D. de Senneville, S. Roujol, C. Moonen, M. Ries, "Motion correction in MR thermometry of abdominal organs: a comparison of the referenceless vs. the multibaseline approach," Magn Reson Med **64**, 1373-1381 (2010).

[258] A.V. Shmatukha, C.J. Bakker, "Correction of proton resonance frequency shift temperature maps for magnetic field disturbances caused by breathing," Phys Med Biol **51**, 4689-4705 (2006).

[259] A.M. El-Sharkawy, M. Schar, P.A. Bottomley, E. Atalar, "Monitoring and correcting spatio-temporal variations of the MR scanner's static magnetic field," MAGMA **19**, 223-236 (2006).

[260] P. Wust, C.H. Cho, B. Hildebrandt, J. Gellermann, "Thermal monitoring: invasive, minimal-invasive and non-invasive approaches," Int J Hyperthermia **22**, 255-262 (2006).

[261] N. McDannold, C. Tempany, F. Jolesz, K. Hynynen, "Evaluation of referenceless thermometry in MRI-guided focused ultrasound surgery of uterine fibroids," J Magn Reson Imaging **28**, 1026-1032 (2008).

[262] V. Rieke, K.K. Vigen, G. Sommer, B.L. Daniel, J.M. Pauly, K. Butts, "Referenceless PRF shift thermometry," Magn Reson Med **51**, 1223-1231 (2004).

[263] K. Kuroda, D. Kokuryo, E. Kumamoto, K. Suzuki, Y. Matsuoka, B. Keserci, "Optimization of self-reference thermometry using complex field estimation," Magn Reson Med **56**, 835-843 (2006).

[264] S.J. Graham, G.J. Stanisz, A. Kecojevic, M.J. Bronskill, R.M. Henkelman, "Analysis of changes in MR properties of tissues after heat treatment," Magn Reson Med **42**, 1061-1071 (1999).

[265] M.A. Jacobs, E.H. Herskovits, H.S. Kim, "Uterine fibroids: diffusion-weighted MR imaging for monitoring therapy with focused ultrasound surgery--preliminary study," Radiology **236**, 196-203 (2005).

[266] S.J. Graham, M.J. Bronskill, R.M. Henkelman, "Time and temperature dependence of MR parameters during thermal coagulation of ex vivo rabbit muscle," Magn Reson Med **39**, 198-203 (1998).

[267] K. Hynynen, A. Darkazanli, C.A. Damianou, E. Unger, J.F. Schenck, "The usefulness of a contrast agent and gradient-recalled acquisition in a steady-state imaging sequence for magnetic resonance imaging-guided noninvasive ultrasound surgery," Invest Radiol **29**, 897-903 (1994).

[268] T. Wu, J.P. Felmlee, J.F. Greenleaf, S.J. Riederer, R.L. Ehman, "Assessment of thermal tissue ablation with MR elastography," Magn Reson Med **45**, 80-87 (2001).

[269] Y. Le, K. Glaser, O. Rouviere, R. Ehman, J.P. Felmlee, "Feasibility of simultaneous temperature and tissue stiffness detection by MRE," Magn Reson Med **55**, 700-705 (2006).

[270] I.J. Rowland, I. Rivens, L. Chen, C.H. Lebozer, D.J. Collins, G.R. ter Haar, M.O. Leach, "MRI study of hepatic tumours following high intensity focused ultrasound surgery," Br J Radiol **70**, 144-153 (1997).

[271] L. Chen, G. ter Haar, D. Robertson, J.P. Bensted, C.R. Hill, "Histological study of normal and tumor-bearing liver treated with focused ultrasound," Ultrasound Med Biol **25**, 847-856 (1999).

[272] H.L. Cheng, C.M. Purcell, J.M. Bilbao, D.B. Plewes, "Prediction of subtle thermal histopathological change using a novel analysis of Gd-DTPA kinetics," J Magn Reson Imaging **18**, 585-598 (2003).

[273] O. Noterdaeme, T.A. Leslie, J.E. Kennedy, R.R. Phillips, M. Brady, "The use of time to maximum enhancement to indicate areas of ablation following the treatment of liver tumours with high-intensity focused ultrasound," Br J Radiol. **82**, 412-420. doi: 410.1259/bjr/18470679. (2009).

[274] F.M. Fennessy, C.M. Tempany, "MRI-guided focused ultrasound surgery of uterine leiomyomas," Acad Radiol **12**, 1158-1166 (2005).

[275] M. Port, J.M. Idee, C. Medina, C. Robic, M. Sabatou, C. Corot, "Efficiency, thermodynamic and kinetic stability of marketed gadolinium chelates and their possible clinical consequences: a critical review," Biometals : an international journal on the role of metal ions in biology, biochemistry, and medicine **21**, 469-490 (2008).

[276] W.P. Cacheris, S.C. Quay, S.M. Rocklage, "The relationship between thermodynamics and the toxicity of gadolinium complexes," Magnetic resonance imaging **8**, 467-481 (1990).

[277] M.C. Pilatou, E.A. Stewart, S.E. Maier, F.M. Fennessy, K. Hynynen, C.M. Tempany, N. McDannold, "MRI-based thermal dosimetry and diffusion-weighted imaging of MRI-guided focused ultrasound thermal ablation of uterine fibroids," J Magn Reson Imaging **29**, 404-411 (2009).

[278] M.A. Jacobs, R. Ouwerkerk, I. Kamel, P.A. Bottomley, D.A. Bluemke, H.S. Kim, "Proton, diffusion-weighted imaging, and sodium (23Na) MRI of uterine leiomyomata after MR-guided high-intensity focused ultrasound: a preliminary study," J Magn Reson Imaging **29**, 649-656 (2009).

[279] J. Chen, B.L. Daniel, C.J. Diederich, D.M. Bouley, M.A. van den Bosch, A.M. Kinsey, G. Sommer, K.B. Pauly, "Monitoring prostate thermal therapy with diffusion-weighted MRI," Magn Reson Med **59**, 1365-1372 (2008).

[280] R. Souchon, O. Rouviere, A. Gelet, V. Detti, S. Srinivasan, J. Ophir, J.Y. Chapelon, "Visualisation of HIFU lesions using elastography of the human prostate in vivo: preliminary results," Ultrasound Med Biol **29**, 1007-1015 (2003).

[281] T. Wu, J.P. Felmlee, J.F. Greenleaf, S.J. Riederer, R.L. Ehman, "MR imaging of shear waves generated by focused ultrasound," Magn Reson Med **43**, 111-115 (2000).

[282] R. Souchon, R. Salomir, O. Beuf, L. Milot, D. Grenier, D. Lyonnet, J.Y. Chapelon, O. Rouviere, "Transient MR elastography (t-MRE) using ultrasound radiation force: theory, safety, and initial experiments in vitro," Magn Reson Med **60**, 871-881 (2008).

[283] M.R. Horsman, R. Murata, J. Overgaard, "Improving local tumor control by combining vascular targeting drugs, mild hyperthermia and radiation," Acta Oncol **40**, 497-503 (2001).

[284] M.L. Hauck, S.M. LaRue, W.P. Petros, J.M. Poulson, D. Yu, I. Spasojevic, A.F. Pruitt, A. Klein, B. Case, D.E. Thrall, D. Needham, M.W. Dewhirst, "Phase I trial of doxorubicin-containing low temperature sensitive liposomes in spontaneous canine tumors," Clinical cancer research : an official journal of the American Association for Cancer Research **12**, 4004-4010 (2006).

[285] S. Dromi, V. Frenkel, A. Luk, B. Traughber, M. Angstadt, M. Bur, J. Poff, J. Xie, S.K. Libutti, K.C. Li, B.J. Wood, "Pulsed-high intensity focused ultrasound and low temperature-sensitive liposomes for enhanced targeted drug delivery and antitumor effect," Clinical cancer research : an official journal of the American Association for Cancer Research **13**, 2722-2727 (2007).

[286] A.W. el-Kareh, T.W. Secomb, "Theoretical models for drug delivery to solid tumors," Crit Rev Biomed Eng **25**, 503-571 (1997).

[287] A.W. El-Kareh, T.W. Secomb, "A mathematical model for comparison of bolus injection, continuous infusion, and liposomal delivery of doxorubicin to tumor cells," Neoplasia **2**, 325-338 (2000).

Publication I

Partanen A, Yarmolenko PS, Viitala A, Appanaboyina S, Haemmerich D, Ranjan A, Jacobs G, Woods D, Enholm J, Wood BJ, Dreher MR, "*Mild hyperthermia with magnetic resonance-guided high-intensity focused ultrasound for applications in drug delivery*," Int J Hyperthermia. 2012;28(4):320-36.

Publication II

Partanen A, Tillander M, Yarmolenko PS, Wood BJ, Dreher MR, Köhler M, "*Reduction of peak acoustic pressure and shaping of heated region by use of multifoci sonications in MR-guided high-intensity focused ultrasound mediated mild hyperthermia*,"
Med Phys. 2013 Jan;40(1):013301

Publication III

Ranjan A, Jacobs GC, Woods DL, Negussie AH, Partanen A, Yarmolenko PS, Gacchina CE, Sharma KV, Frenkel V, Wood BJ, Dreher MR, "*Image-guided drug delivery with magnetic resonance guided high intensity focused ultrasound and temperature sensitive liposomes in a rabbit Vx2 tumor model*," J Control Release. 2012 Mar 28;158(3):487-94.

Publication IV

Negussie AH, Yarmolenko PS, Partanen A, Ranjan A, Jacobs G, Woods D, Bryant H, Thomasson D, Dewhirst MW, Wood BJ, Dreher MR, "*Formulation and characterisation of magnetic resonance imageable thermally sensitive liposomes for use with magnetic resonance-guided high intensity focused ultrasound*," Int J Hyperthermia. 2011;27(2):140-55.

Publication V

Gasselhuber A, Dreher MR, Partanen A, Yarmolenko PS, Woods D, Wood BJ, Haemmerich D, "*Targeted drug delivery by high intensity focused ultrasound mediated hyperthermia combined with temperature-sensitive liposomes: computational modelling and preliminary in vivo validation*," Int J Hyperthermia. 2012;28(4):337-48.

Publication VI

Venkatesan AM, Partanen A, Pulanic TK, Dreher MR, Fischer J, Zurawin RK, Muthupillai R, Sokka S, Nieminen HJ, Sinaii N, Merino M, Wood BJ, Stratton P, "*Magnetic resonance imaging-guided volumetric ablation of symptomatic leiomyomata: correlation of imaging with histology*," J Vasc Interv Radiol. 2012 Jun;23(6):786-794.

ISBN 978-952-10-8094-4 (pbk.)
ISBN 978-952-10-8095-1 (PDF)
ISSN 0356-0961
E-thesis http://ethesis.helsinki.fi

Helsinki University Print
Helsinki, 2013